

QCD sum rule analysis of Heavy Quarkonia in magnetized matter - effects of (inverse) magnetic catalysis

Pallabi Parui,^{*} Sourodeep De,[†] Ankit Kumar,[‡] and Amruta Mishra[§]

Department of Physics, Indian Institute of Technology, Delhi, New Delhi - 110016

Abstract

In-medium masses of the $1S$ and $1P$ states of heavy quarkonia are investigated in the magnetized, asymmetric nuclear medium, accounting for the Dirac sea effects, using a combined approach of chiral effective model and QCD sum rule method. Masses are calculated from the in-medium scalar and twist-2 gluon condensates, calculated within the chiral model. The gluon condensate is simulated through the scalar dilaton field, χ introduced in the model through a scale-invariance breaking logarithmic potential. The contribution of Dirac sea is incorporated through the nucleonic tadpole diagrams. Considering the scalar fields to be classical, the dilaton field, χ , the non-strange isoscalar, $\sigma(\sim (\langle \bar{u}u \rangle + \langle \bar{d}d \rangle))$, strange isoscalar, $\zeta(\sim \langle \bar{s}s \rangle)$ and non-strange isovector, $\delta(\sim (\langle \bar{u}u \rangle - \langle \bar{d}d \rangle))$ fields, are obtained by solving their coupled equations of motion, as derived from the chiral model Lagrangian. The effects of magnetic field are taken into account through the Dirac sea as well as the Landau energy levels of protons, and the non-zero anomalous magnetic moments of the nucleons. The scalar fields modify appreciably with magnetic field, due to the Dirac sea contribution, in comparison to the case when only Landau level contribution is there. Thus, in-medium masses of the charmonium and bottomonium ground states are observed to have appreciable modifications with magnetic field due to the Dirac sea contributions. In presence of an external magnetic field, there is mixing between the longitudinal component of the vector meson and pseudoscalar meson (PV mixing) in both quarkonia sectors, leading to a rise (drop) of the masses of J/ψ^{\parallel} (η_c) and $\Upsilon^{\parallel}(1S)$ (η_b) states. These might show in the experimental observables, e.g., the dilepton spectra in the non-central, ultra-relativistic heavy ion collision experiments at RHIC and LHC, where the produced magnetic field is huge.

^{*}Electronic address: pallabiparui123@gmail.com

[†]Electronic address: sourodeepde2015@gmail.com

[‡]Electronic address: ankitchahal17795@gmail.com

[§]Electronic address: amruta@physics.iitd.ac.in

I. INTRODUCTION

The study of the in-medium properties of hadrons is an important area of research in the physics of strongly interacting matter. The study of the heavy flavor hadrons [1] has attracted a lot of attention due to its relevance in the ultra-relativistic heavy ion collision experiments. Recently, heavy quarkonia ($\bar{q}q$; $q = c, b$) under extreme conditions of matter i.e., high density and/or high temperature, have been investigated extensively. The medium created in the relativistic, high energy collisions between the heavy ions beams, affect the masses and decay widths of the produced particles in such collisions, which can have significant observable impacts, e.g., in the production and propagation of the particles. In the non-central heavy ion collision experiments, strong magnetic fields are expected to be produced [2–5]. The produced magnetic fields have been estimated to be huge at RHIC in BNL and at LHC in CERN [6]. However, the time evolution of the produced magnetic field in such collisions, requires the detailed knowledge of the electrical conductivity of the medium and proper treatment of the solutions of magneto-hydrodynamic equations [6], which is still an open question. The study of the effects of strong magnetic fields on the in-medium properties of hadrons has initiated a new area of research in the physics of heavy ion collisions. The heavy quarkonia are the bound states of a heavy quark ($q = c$ or, b) and its antiquark. Charmonium ($\bar{c}c$) and bottomonium ($\bar{b}b$) states have been investigated in the literature using a variety of approaches, i.e., the potential models [7–9], the QCD sum rule approach [10–15], the coupled channel approach [16], quark-meson coupling model [17, 18], a chiral effective model [19–21], and a field theoretic model for composite hadrons [22, 23]. In the present work, we study the in-medium masses of the $1S$ -wave (vector, J/ψ , pseudoscalar, η_c) and $1P$ -wave (scalar, χ_{c0} , axial-vector, χ_{c1}) charmonium states as well as the $1S$ -wave (vector, $\Upsilon(1S)$, pseudoscalar, η_b) and $1P$ -wave (scalar, χ_{b0} , axial-vector, χ_{b1}) bottomonium states, in a magnetized, isospin asymmetric nuclear medium, using the QCD sum rule approach, by incorporating the effect of Dirac sea in presence of an external magnetic field. At finite magnetic field, effects of PV mixing between the longitudinal component of the vector state, J/ψ^{\parallel} ($\Upsilon^{\parallel}(1S)$) and the pseudoscalar state, η_c (η_b) are studied in both quarkonia sector. The ground states ($1S$ and $1P$) of charmonium and bottomonium have been studied within the magnetized nuclear matter, without accounting for the Dirac sea effects [14, 15, 24], by the QCD sum rule method. The medium modifications are studied through the QCD gluon

condensates [25], in terms of the medium modifications of a scalar dilaton field, χ , within the chiral SU(3) model. In our present study, we have considered the effects of magnetized Dirac sea in addition to the Landau levels contributions of protons, in the magnetic (nuclear) medium, within the chiral SU(3) model. The effects of magnetic fields on the scalar fields, which correspond to the light quark condensates, are seen to be important due to the magnetized Dirac sea contributions. The enhancement of these quark condensates with rising magnetic field, is called magnetic catalysis [26–29]. In the literature, this effect has been studied in a large extent on the quark matter sector using the Nambu-Jona-Lasinio (NJL) model [30–32]. In ref.[33], the effects of magnetic catalysis have been studied in the context of nuclear matter, through the contributions of magnetized Dirac sea on the free energy density. The Walecka model and an extended linear sigma model have been used to study the effects of magnetic catalysis on the nuclear matter phase transition. The magnetic catalysis effect is observed indirectly through a rise in the scalar field $\sigma(\sim \langle \bar{q}q \rangle)$ with magnetic field, at zero temperature and at zero baryon density, without considering the anomalous magnetic moments of the nucleons. The effective nucleon mass, $m_N^* = m_N - g_{\sigma N}\sigma$, increases with rising magnetic field at zero density and zero temperature, as a consequence of the magnetic catalysis effect, where, m_N is the vacuum mass of the nucleon and $g_{\sigma N}$, the σ -nucleon coupling constant in the Lagrangian. In ref.[34], the effects of an external magnetic field have been studied on the vacuum to nuclear matter phase transition in the Walecka model, by using a weak-field approximation for the fermion propagator. The effects of the anomalous magnetic moments (AMMs) of the nucleons are observed to lead to an enhanced magnetic catalysis effect through the rise of the effective nucleon mass (m_N^*) with increasing magnetic field, at zero temperature and at zero baryon density, as compared to the case with zero AMMs of nucleons [34]. However, the critical temperature for the vacuum to nuclear matter phase transition for the nonzero AMMs of the nucleons, are seen to decrease with increasing magnetic field, implying an inverse magnetic catalysis effect [35]. Whereas for zero anomalous magnetic moments of the nucleons, the behavior is opposite, indicating the magnetic catalysis. The contributions of the magnetized Dirac sea have been incorporated through summation over the nucleonic tadpole diagrams, in the weak-field limit of the interacting fermion propagators [34]. In the literature there are very few works regarding the effects of (inverse) magnetic catalysis on the nuclear matter properties. In our work, the effects of (inverse) magnetic catalysis are to be studied by investigating the contributions of Dirac sea

on the scalar fields of the chiral model, in the presence of an external magnetic field. The in-medium masses of the open heavy flavor mesons, namely the open charm and open bottom mesons, have been studied within the QCD sum rule approach [36–38], and using the generalized version of the chiral effective model, both in the absence of an external magnetic field [39, 40], and in presence of a magnetic field [41, 42]. The in-medium masses of the light vector mesons (ρ, ω, ϕ) have been studied within the QCD sum rule approach [43]. The medium modifications of the masses obtained from the non-strange ($\langle \bar{q}q \rangle$; $q = u, d$ for ρ, ω) and strange ($\langle \bar{s}s \rangle$ for ϕ) light quark condensates and the scalar gluon condensates ($\sim \langle G_{\mu\nu}^a G^{a\mu\nu} \rangle$), calculated within the chiral $SU(3)$ model, in the strange asymmetric matter, in absence of magnetic field [44], and in the magnetized nuclear medium [45]. In QCD sum rule approach, the mass shifts of the heavy quarkonia (charmonia and bottomonia) are coming through the medium modifications of the scalar gluon and twist-2 gluon condensates, calculated in a chiral effective model. The open heavy flavor mesons have their mass modifications in terms of both the light quark condensates (because of the light quark flavor present in their quark structure) as well as the gluon condensates simulated within the chiral model by the scalar dilaton field, χ . From the in-medium masses of the charmonium (bottomonium) and the open charm (open bottom) mesons, the in-medium partial decay widths of charmonium, $\Psi(3770)$ (bottomonium, $\Upsilon(4S)$) going to $D\bar{D}$ ($B\bar{B}$), have been studied in the presence of an external magnetic field, using a field theoretic model for composite hadrons with quark (and antiquark) constituents [22, 46, 47] and using a light quark-antiquark pair creation model, namely the 3P_0 model [48]. These studies have important observable consequences in the relativistic heavy ion collision experiments, with the current focus on the heavy flavor mesons in magnetized matter [49–51]. There have been finite temperature studies of heavy quarkonia within the QCD sum rule framework [13, 52–54]. The magnetically induced mixing between ($\eta_c - J/\psi^{\parallel}$) have been studied using a phenomenological interaction Lagrangian [22, 24, 51, 55] and including the bottom sector (between $\eta_b - \Upsilon(1S)^{\parallel}$) from the spin-magnetic field interaction Hamilton [14, 15, 56].

In section.II, the chiral effective model is described briefly to calculate the medium modified gluon condensates. Section.III illustrates the QCD Sum Rule framework, to find the in-medium masses of the lowest lying quarkonia; the mass shifts of the S-wave states due to the pseudoscalar-vector (PV) mesons mixing are introduced in presence of a magnetic field. In section.IV, the results of the in-medium masses and their shifts at various conditions of

magnetized nuclear matter are discussed. Section.V presents the summary of this study.

II. THE CHIRAL $SU(3)_L \times SU(3)_R$ MODEL

In-medium masses of the quarkonium ground states are computed within the QCD sum rule approach, in terms of the scalar and twist-2 gluon condensates. In the present study, these condensates are calculated within an effective chiral hadronic model [57]. The chiral model is based on the non-linear realization of chiral $SU(3)_L \times SU(3)_R$ symmetry [58–60], and the broken scale invariance of QCD [57, 61, 62]. An effective Lagrangian, based on the non-linear realization of chiral symmetry is employed here, with a logarithmic potential in the scalar dilaton field, χ [63], which simulates the QCD scale-invariance breaking within the model. The chiral model Lagrangian density has the following general form [57],

$$\mathcal{L} = \mathcal{L}_{kin} + \mathcal{L}_{BM} + \mathcal{L}_{vec} + \mathcal{L}_0 + \mathcal{L}_{scale-break} + \mathcal{L}_{SB} + \mathcal{L}_{mag} \quad (1)$$

in the above expression, \mathcal{L}_{kin} is the kinetic energy of the baryons and the mesons; \mathcal{L}_{BM} represents the baryon-mesons (spin-0 and spin-1) interactions; \mathcal{L}_{vec} , contains the quartic self-interactions of the vector mesons and their couplings with the scalar ones; \mathcal{L}_0 incorporates the spontaneous chiral symmetry breaking effects via meson-meson interactions; $\mathcal{L}_{scale-break}$ is the QCD scale symmetry breaking logarithmic potential; the explicit symmetry breaking term is, \mathcal{L}_{SB} ; finally the magnetic field effects on the charged and neutral baryons in the nuclear medium are given by [19, 20, 41, 42, 64–67],

$$\mathcal{L}_{mag} = -\frac{1}{4}F_{\mu\nu}F^{\mu\nu} - q_i\bar{\psi}_i\gamma_\mu A^\mu\psi_i - \frac{1}{4}\kappa_i\mu_N\bar{\psi}_i\sigma^{\mu\nu}F_{\mu\nu}\psi_i \quad (2)$$

where, ψ_i is the baryon field operator ($i = p, n$, in case of nuclear matter), the parameter, κ_i here is related to the anomalous magnetic moment of the i -th baryon, with $\kappa_p = 3.5856$ and $\kappa_n = -3.8263$, are the gyromagnetic ratio corresponding to the anomalous magnetic moments (AMM) of the proton and the neutron respectively [64–71]. In magnetized nuclear medium, there are contributions from the protons Landau energy levels [68], and the nucleons anomalous magnetic moments [68, 71], to the number and scalar densities ($\rho_i, \rho_i^s, i = p, n$, respectively) of the nucleons [41, 42]. Effects of the magnetized Dirac sea are considered in our present study, to calculate the in-medium masses of the heavy quarkonium ground states. The one-loop self energy functions of the nucleons, evaluated through summation

over the scalars (σ , ζ and δ) and vectors (ρ and ω) tadpole diagrams, using the weak-field expansion of the nucleonic propagator, accounting for the AMMs of nucleons, within the chiral effective model. Therefore, within the chiral $SU(3)$ model, the Dirac sea contributes to the scalar densities of nucleons, at finite magnetic field, incorporating the effects of the anomalous magnetic moments of nucleons.

The meson fields of the chiral model Lagrangian, are treated as the classical fields, whereas the nucleons as the quantum fields, in the evaluation of the Dirac sea contribution to the scalar fields. The scalar dilaton field, χ simulates the scalar gluon condensate $\langle \frac{\alpha_s}{\pi} G_{\mu\nu}^a G^{a\mu\nu} \rangle$, as well as the twist-2 gluon operator $\langle \frac{\alpha_s}{\pi} G_{\mu\sigma}^a G_\nu^{a\sigma} \rangle$, within the model. The energy momentum tensor, $T_{\mu\nu}$ derived from the χ -dependent terms in the chiral model Lagrangian density [13] thus obtained,

$$T_{\mu\nu} = (\partial_\mu \chi) \left(\frac{\partial \mathcal{L}}{\partial (\partial^\nu \chi)} \right) - g_{\mu\nu} \mathcal{L}_\chi \quad (3)$$

The QCD energy momentum tensor, in the limit of finite current quark masses, contains a symmetric trace-less part and a trace part [72, 73],

$$T_{\mu\nu} = -ST (G_{\mu\sigma}^a G_\nu^{a\sigma}) + \frac{g_{\mu\nu}}{4} \left(\sum_i m_i \bar{q}_i q_i + \langle \frac{\beta_{QCD}}{2g} G_{\sigma k}^a G_k^{a\sigma} \rangle \right) \quad (4)$$

with the leading order QCD β function [13], $\beta_{QCD}(g) = -\frac{g^3}{(4\pi)^2} (11 - \frac{2}{3} N_f)$, by taking the 3 color quantum numbers of QCD, and no. of flavors, $N_f = 3$. Here, m_i 's ($i = u, d, s$) are the current quark masses. The medium expectation value of the twist-2 gluon operator is,

$$\langle \frac{\alpha_s}{\pi} G_{\mu\sigma}^a G_\nu^{a\sigma} \rangle = \left(u_\mu u_\nu - \frac{g_{\mu\nu}}{4} \right) G_2 \quad (5)$$

where u_μ is the 4-velocity of the nuclear medium, taken to be at rest [13, 14] in the present investigation, namely, $u_\mu = (1, 0, 0, 0)$. The energy momentum tensor of QCD thus reads

$$T_{\mu\nu} = -\frac{\pi}{\alpha_s} \left(u_\mu u_\nu - \frac{g_{\mu\nu}}{4} \right) G_2 + \frac{g_{\mu\nu}}{4} \left(\sum_i m_i \bar{q}_i q_i + \langle \frac{\beta_{QCD}}{2g} G_{\sigma k}^a G_k^{a\sigma} \rangle \right) \quad (6)$$

Comparing the expressions of energy momentum tensor from equation(6) and equation(3), the expressions for G_2 (the twist-2 component) and the scalar gluon condensate are given by multiplying both sides with $(u_\mu u_\nu - \frac{g_{\mu\nu}}{4})$ and $g^{\mu\nu}$ respectively. These are given by-

$$G_2 = \frac{\alpha_s}{\pi} \left[- (1 - d + 4k_4)(\chi^4 - \chi_0^4) - \chi^4 \ln \left(\frac{\chi^4}{\chi_0^4} \right) + \frac{4}{3} d \chi^4 \ln \left(\left(\frac{(\sigma^2 - \delta^2)\zeta}{\sigma_0^2 \zeta_0} \right) \left(\frac{\chi}{\chi_0} \right)^3 \right) \right] \quad (7)$$

and,

$$\langle \frac{\alpha_s}{\pi} G_{\mu\nu}^a G^{a\mu\nu} \rangle = \frac{8}{9} \left[(1-d)\chi^4 + \left(\frac{\chi}{\chi_0} \right)^2 \left(m_\pi^2 f_\pi \sigma + \left(\sqrt{2} m_k^2 f_k - \frac{1}{\sqrt{2}} m_\pi^2 f_\pi \right) \zeta \right) \right] \quad (8)$$

The expectation values of the scalar and the twist-2 gluon condensates in magnetized nuclear medium, depend on the in-medium values of the non-strange scalar-isoscalar field, σ , strange scalar-isoscalar field, ζ , scalar-isovector field, δ and the scalar dilaton field, χ , within the chiral $SU(3)$ model. The Euler Lagrange's equations of motion corresponding to the fields are derived from the chiral effective Lagrangian. The contributions of magnetic fields on the scalar fields are obtained through the scalar and number densities of the nucleons, which are modified due to the Landau energy levels of protons and the anomalous magnetic moments of nucleons. The magnetized Dirac sea also contributes to the scalar densities of nucleons and hence on the scalar fields, at zero and finite density matter.

III. IN-MEDIUM MASSES WITHIN THE QCD SUM RULE APPROACH

The in-medium masses of the $1S$ -wave and $1P$ -wave states of charmonium [$1S$: J/ψ , η_c and $1P$: χ_{c0} , χ_{c1}] and bottomonium [$1S$: $\Upsilon(1S)$, η_b and $1P$: χ_{b0} , χ_{b1}] are studied within the QCD Sum Rule approach. In this approach, masses of the heavy-quarkonium ground states are calculated in terms of the medium modified scalar and twist-2 gluon condensates. The condensates are obtained within the chiral model, through the in-medium values of the scalar fields in the magnetized, asymmetric nuclear matter with the additional contribution from the magnetized Dirac sea. The in-medium mass squared, m_i^{*2} of the i -type of quarkonium ground state (i = vector, pseudoscalar, scalar, and axial-vector) is given as [74],

$$m_i^{*2} \simeq \frac{M_{n-1}^i(\xi)}{M_n^i(\xi)} - 4m_q^2 \xi \quad (9)$$

where M_n^i is the n -th moment of the i -type meson state and m_q ($q = c, b$) is the running heavy quark mass, dependent on the renormalization scale, ξ . The expressions for the running charm and bottom quark masses are given later. Using the operator product expansion technique [OPE], the moment can be written as [10, 74],

$$M_n^i(\xi) = A_n^i(\xi) \left[1 + a_n^i(\xi) \alpha_s + b_n^i(\xi) \phi_b + c_n^i(\xi) \phi_c \right] \quad (10)$$

where A_n^i , a_n^i , b_n^i , and c_n^i are the Wilson coefficients. The coefficients, A_n^i result from the bare-loop diagram of perturbative QCD, a_n^i are the contributions of the perturbative radiative

corrections, and b_n^i are related to the scalar gluon condensate through

$$\phi_b = \frac{4\pi^2}{9} \frac{\langle \frac{\alpha_s}{\pi} G_{\mu\nu}^a G^{a\mu\nu} \rangle}{(4m_q^2)^2}. \quad (11)$$

By substituting the expression for the scalar gluon condensate from equation (8),

$$\phi_b = \frac{32\pi^2}{81 (4m_q^2)^2} \left[(1-d)\chi^4 + \left(\frac{\chi}{\chi_0} \right)^2 \left(m_\pi^2 f_\pi \sigma + \left(\sqrt{2} m_k^2 f_k - \frac{1}{\sqrt{2}} m_\pi^2 f_\pi \right) \zeta \right) \right] \quad (12)$$

The coefficients c_n^i are associated with the twist-2 gluon condensates as

$$\phi_c = \frac{4\pi^2}{3 (4m_q^2)^2} G_2 \quad (13)$$

which using equation (7), reduces to

$$\phi_c = \frac{4\pi\alpha_s}{3 (4m_q^2)^2} \left[- (1-d+4k_4)(\chi^4 - \chi_0^4) - \chi^4 \ln \left(\frac{\chi^4}{\chi_0^4} \right) + \frac{4}{3} d \chi^4 \ln \left(\frac{(\sigma^2 - \delta^2)\zeta\chi^3}{\sigma_0^2 \zeta_0 \chi_0^3} \right) \right] \quad (14)$$

The ξ -dependent parameters m_q , ($q = c, b$) and the running coupling constant, α_s are [13, 74]

$$\frac{m_q(\xi)}{m_q} = 1 - \frac{\alpha_s}{\pi} \left[\frac{2+\xi}{1+\xi} \ln(2+\xi) - 2 \ln 2 \right] \quad (15)$$

with $m_c \equiv m_c(p^2 = -m_c^2) = 1.26$ GeV and $m_b \equiv m_b(p^2 = -m_b^2) = 4.23$ GeV [13, 75], and

$$\alpha_s(Q_0^2 + 4m_q^2) = \alpha_s(4m_q^2) \left/ \left(1 + \frac{(33-2n_f)}{12\pi} \alpha_s(4m_q^2) \ln \frac{Q_0^2 + 4m_q^2}{4m_q^2} \right) \right. \quad (16)$$

with $Q_0^2 = 4m_q^2 \xi$ ($q = c, b$), and $n_f = 4$, $\alpha_s(4m_c^2) \simeq 0.23$ in the charm quark sector, and $n_f = 5$, $\alpha_s(4m_b^2) \simeq 0.15$ in the bottom quark sector [75].

The Wilson coefficients, A_n^i , a_n^i and b_n^i are given in ref.[74] for different J^{PC} quantum numbers of states, for e.g., the pseudoscalar, vector, scalar, axial-vector channels. The c_n^i s' are listed for the vector and pseudoscalar ($1S$ states) channels in ref.[10], and for the $1P$ -wave states (scalar and axial-vector), c_n^i s' are calculated using a background field technique [53].

At finite magnetic field, mixing of the pseudoscalar ($P \equiv \eta_c(1S)$) and vector ($V \equiv J/\psi$) charmonium states are considered through the interaction Lagrangian [22, 24, 38, 47, 55]

$$\mathcal{L}_{PV\gamma} = \frac{g_{PV}}{m_{av}} e \tilde{F}_{\mu\nu} (\partial^\mu P) V^\nu, \quad (17)$$

where $m_{av} = (m_V + m_P)/2$, m_P and m_V are the masses for the pseudoscalar and vector charmonium states, $\tilde{F}_{\mu\nu}$ is the dual electromagnetic field strength tensor. In equation (17), the coupling parameter g_{PV} is fitted from the observed value of the radiative decay width,

$$\Gamma(V \rightarrow P\gamma) = \frac{e^2}{12} \frac{g_{PV}^2 p_{cm}^3}{\pi m_{av}^2}, \quad (18)$$

where, $p_{cm} = (m_V^2 - m_P^2)/(2m_V)$ is the magnitude of the center of mass momentum in the final state. The masses of the pseudoscalar and the longitudinal component of the vector mesons including the mixing effects are given by

$$m_{P,V\parallel}^2 (PV) = \frac{1}{2} \left(M_+^2 + \frac{c_{PV}^2}{m_{av}^2} \mp \sqrt{M_-^4 + \frac{2c_{PV}^2 M_+^2}{m_{av}^2} + \frac{c_{PV}^4}{m_{av}^4}} \right), \quad (19)$$

where $M_+^2 = m_P^2 + m_V^2$, $M_-^2 = m_V^2 - m_P^2$ and $c_{PV} = g_{PV}eB$. Considering the terms in equation (19) up to the second order in c_{PV} and leading order in $(m_V - m_P)/2m_{av}$, we get

$$m_{P,V\parallel}^2 (PV) = m_{P/V}^2 \mp \frac{c_{PV}^2}{M_-^2} \quad (20)$$

The effective Lagrangian given by equation (17) is observed to lead to the mass modifications of the longitudinal J/ψ and η_c states in the presence of magnetic field, which agree extremely well with a study of these charmonium states using a QCD sum rule approach incorporating the mixing effects [24, 55]. In the present study, we have incorporated the effects from the magnetized Dirac sea, apart from the Landau level contributions of the Fermi sea of protons, in the PV mixing calculation of the longitudinal component of vector ($J/\psi\parallel$) and the pseudoscalar (η_c) states of charmonium. The in-medium masses, m_V and m_P are calculated from the QCD sum rule approach, described above. Effects of spin-magnetic field interaction have been studied for the 1S charmonium states ($J/\psi\parallel$ - η_c) at finite magnetic fields [14, 24, 51, 55, 56]. This leads to a level repulsion between the masses of $J/\psi\parallel$ and η_c .

The contribution of magnetic field through the spin-magnetic field interaction are considered on the 1S triplet and singlet states of bottomonium. The spin-magnetic coupling leads to a mixing between the longitudinal component of the vector ($\Upsilon\parallel(1S)$) and the pseudoscalar (η_b) states. The spin-mixing effects are studied, including the additional contribution of the magnetized Dirac sea on the masses. The effective masses of $\Upsilon\parallel(1S)$ and η_b , by considering the shifts due to the spin-magnetic field interaction, $-\mu_s B$ [56], are given by

$$m_{\Upsilon(1S)}^{eff} = m_{\Upsilon(1S)}^* + \Delta m_{sB}, \quad m_{\eta_b}^{eff} = m_{\eta_b}^* - \Delta m_{sB} \quad (21)$$

In the above equation, $m_{\Upsilon(1S)/\eta_b}^*$ denotes the in-medium masses of the S-wave bottomonium ground states calculated within QCD sum rule framework [equation (9)], and Δm_{sB} is the shift due to the spin-magnetic field interaction, given by

$$\Delta m_{sB} = \frac{\Delta M}{2} \left((1 + \chi_{sB}^2)^{1/2} - 1 \right), \quad \chi_{sB} = \frac{2g\mu_b B}{\Delta M} \quad (22)$$

where, $\mu_b = (\frac{1}{3}e)/(2m_b)$ is the bottom quark Bohr magneton with the constituent bottom quark mass, $m_b = 4.7$ GeV [56], $\Delta M = m_\Upsilon^* - m_{\eta_b}^*$, and g is chosen to be 2 (ignoring the anomalous magnetic moments of the bottom quark (anti-quark)). The Hamiltonian approach is taken to study the spin-mixing effects in the bottomonium sector (unlike $\bar{c}c$), due to the lack of experimental data on the bottomonium radiative decay width, $\Upsilon(1S) \rightarrow \eta_b\gamma$.

IV. RESULTS AND DISCUSSIONS

A. Charmonium states

In this subsection, the results for the in-medium masses of the lowest S -wave: J/ψ (3S_1), η_c (1S_0) and P -wave: χ_{c0} (3P_0), χ_{c1} (3P_1), states of charmonium are discussed in the presence of magnetized, asymmetric nuclear matter, accounting for the effects of magnetized Dirac sea (denoted as DS). In the sum rule approach, masses are obtained by calculating the moments (M_n^i) for all the four currents: vector (3S_1), pseudoscalar (1S_0), scalar (3P_0) and axial-vector (3P_1). The moments, M_n^i , are given in terms of the perturbative Wilson coefficients and the non-perturbative gluon condensates of QCD, as given by equation (10). Wilson coefficients are calculated for different J^{PC} quantum numbers of the currents and are independent of the medium effects [10, 53, 74]. The mass formula in the sum rule framework [equation (9)], depends on the running charm quark mass, $m_c(\xi)$, and the running coupling constant, $\alpha_s(\xi)$, which are functions of the renormalization scale ξ , given by equations (15) and (16) respectively. The scalar gluon condensate, $\langle \frac{\alpha_s}{\pi} G_{\mu\nu}^a G^{a\mu\nu} \rangle$ is connected to the ϕ_b term, whereas, the twist-2 gluon condensate, G_2 to the ϕ_c term, which incorporate the medium effects in the mass calculation. The gluon condensates are obtained from the chiral effective model [equations (7) and (8)]. In presence of an external magnetic field, in the nuclear matter, the Landau level contributions of charged particles (protons) and the anomalous magnetic moments (AMMs) of neutrons and protons lead to the modifications of the number and scalar densities of nucleons ($\rho_i, \rho_i^s; i = p, n$) [41, 42, 64, 65]. In the present investigation, the effects of the magnetized Dirac sea are taken into account through the scalar densities of protons (ρ_p^s) and neutrons (ρ_n^s). Therefore, within the chiral $SU(3)$ model, the coupled equations of motion in the scalar fields are solved accounting for the protons Landau energy levels and the Dirac sea contribution at finite magnetic field, for the given values of baryon

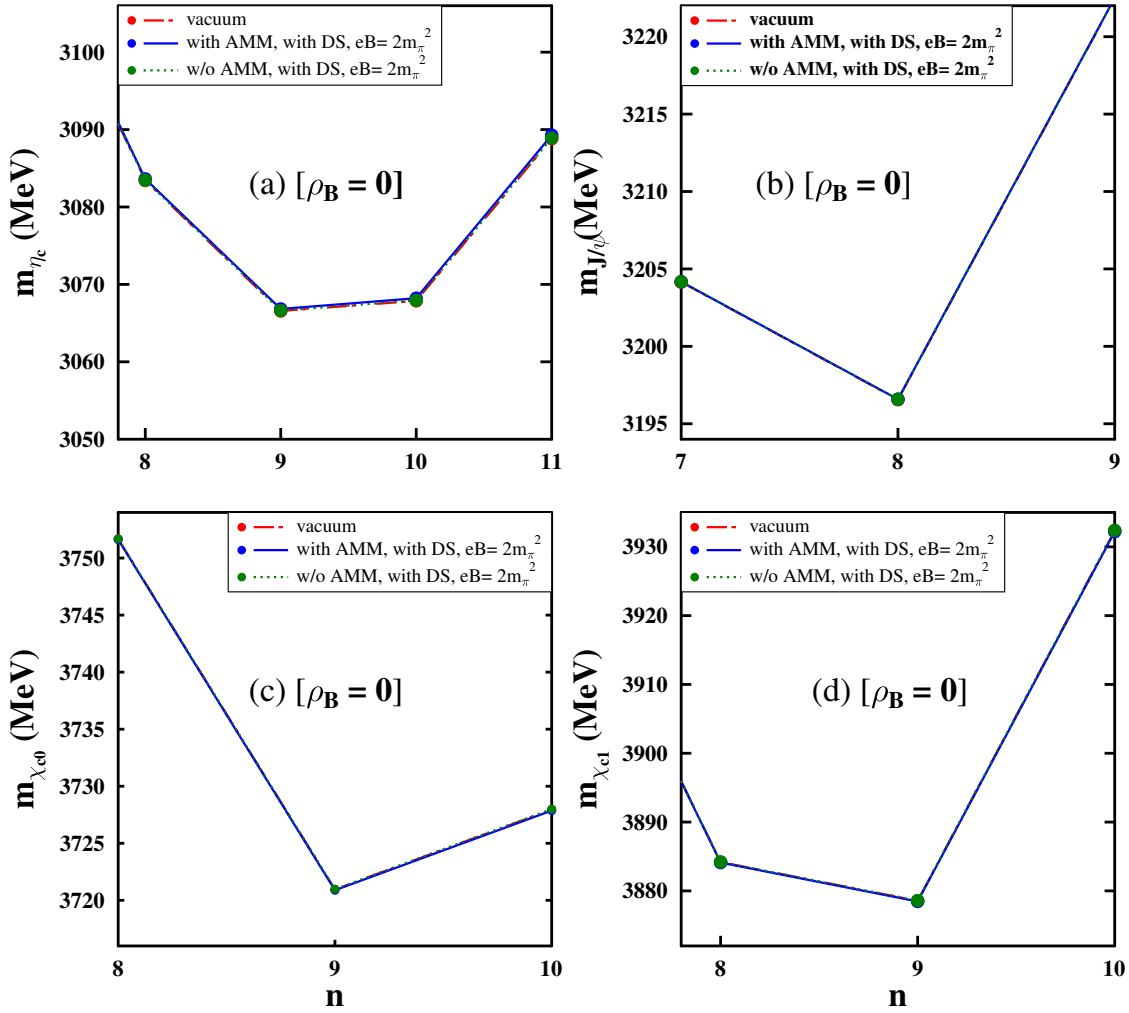


FIG. 1: Masses (in MeV) are plotted as functions of n , for $1S$ (J/ψ , η_c) and $1P$ (χ_{c0} and χ_{c1}) states of charmonium, at $\rho_B = 0$. Dirac sea (DS) effects are considered at $eB = 2m_\pi^2$, with and without the nucleons anomalous magnetic moments (AMMs).

density, ρ_B , isospin asymmetry parameter, $\eta = (\rho_n - \rho_p)/2\rho_B$, (ρ_p and ρ_n are the number densities of proton and neutron, respectively) and magnetic field, $|eB|$ (in units of m_π^2). The effects of Dirac sea in the magnetized nuclear matter, lead to the appreciable changes in the values of the scalar fields. As the light quark condensates are related to the scalar fields, the enhancement (diminution) in the values of the scalar fields with magnetic field, indirectly indicate (inverse) magnetic catalysis. The effects of the Dirac sea are taken into account through summation of the scalar (σ , ζ and δ) and vector (ρ and ω) mesons tadpole diagrams in the evaluation of nucleonic one-loop self energy functions, using the weak-field

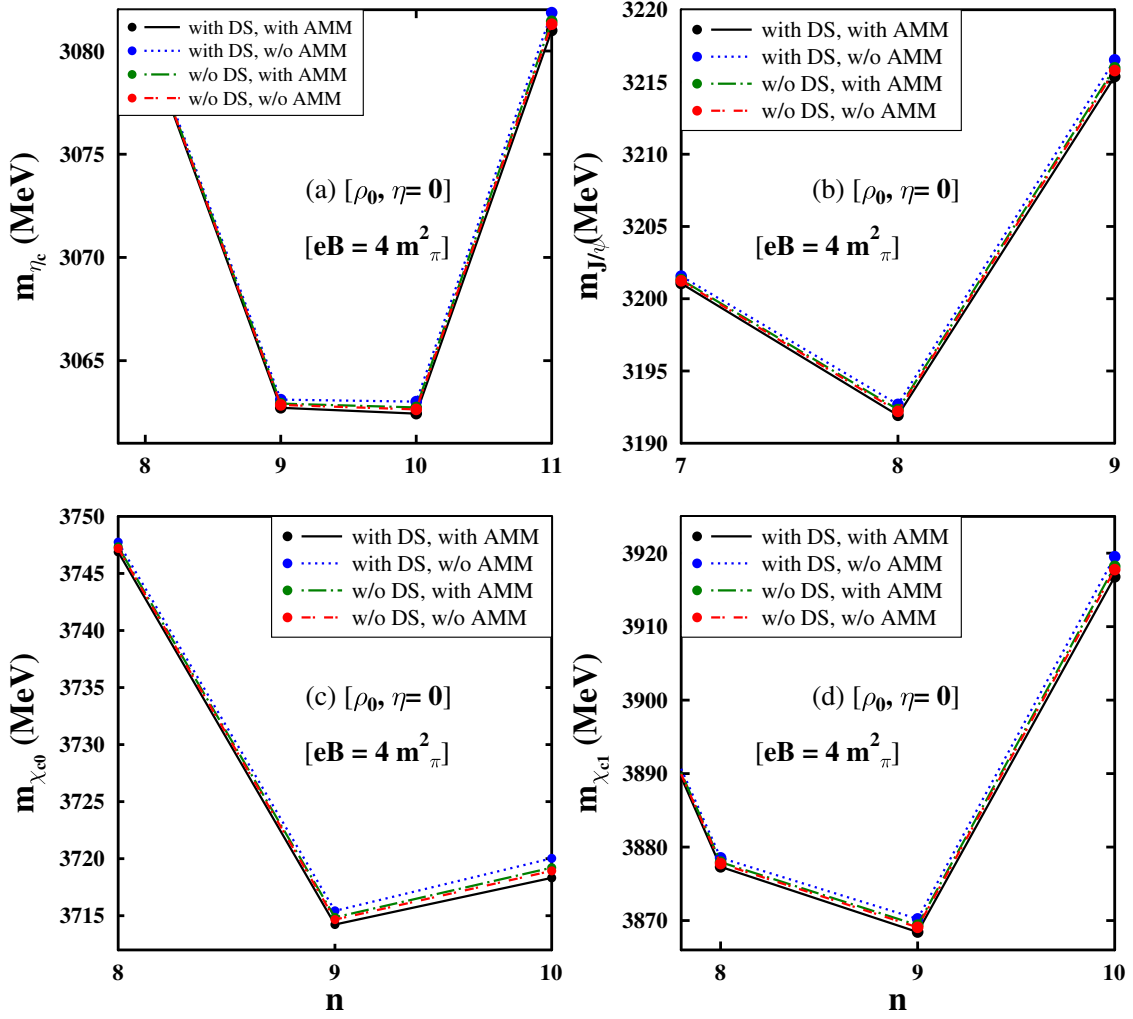


FIG. 2: Masses (MeV) are plotted as functions of n , for J/ψ , η_c , χ_{c0} and χ_{c1} , at ρ_0 , $\eta = 0$. Contributions of the Dirac sea (DS), Landau quantization of protons, and nucleons AMMs, at $eB = 4m_\pi^2$, are considered. Comparison are made when the effects of DS and nucleons AMMs, are not taken into account.

approximation of the fermion propagators, within the chiral effective model. The Dirac sea contributes to the scalar densities of the nucleons, which is implemented in the scalar fields of the chiral effective model by solving their coupled equations of motion. In the presence of an external magnetic field, the mixing between the longitudinal component of the vector and the pseudoscalar states of charmonium are studied using a phenomenological Lagrangian approach, accounting for the additional effects of Dirac sea. The effective masses of J/ψ^{\parallel} and η_c thus given by equation (20). The nuclear matter saturation density, ρ_0 is taken to

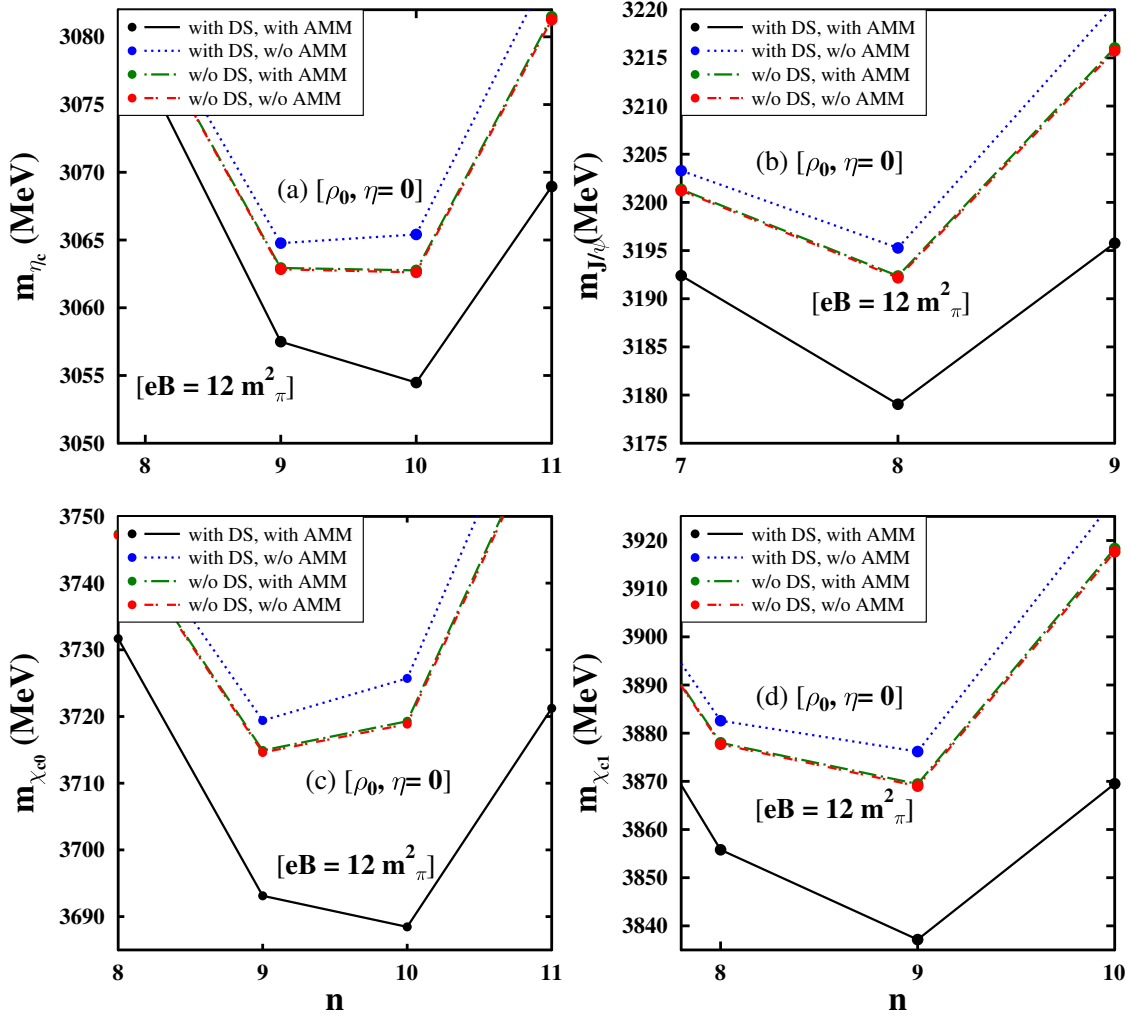


FIG. 3: Masses (MeV) are plotted as functions of n , for J/ψ , η_c , χ_{c0} and χ_{c1} at $\rho_B = \rho_0$, $\eta = 0$. Contributions of the Dirac sea (DS), Landau quantization of protons, and nucleons AMMs, at $eB = 12m_\pi^2$, are considered. Comparison are made when effects of DS and nucleons AMMs, are not taken into account.

be 0.15 fm^{-3} in the present work.

The value of the renormalization scale, $\xi = 1$ is chosen for the S -wave charmonium states and $\xi = 2.5$ for the P -wave charmonium states, to study their respective in-medium masses. These choices lead to the ξ dependent coupling constant and charm quark mass, $\alpha_s = 0.21$ and $m_c = 1.24 \text{ GeV}$ for the $1S$ states and $\alpha_s = 0.1948$ and $m_c = 1.22 \text{ GeV}$ for the $1P$ states of charmonium. Using these parameters and ϕ_b in terms of the scalar gluon condensate, $\langle \frac{\alpha_s}{\pi} G_{\mu\nu}^a G^{a\mu\nu} \rangle$, calculated within the chiral effective model, the vacuum masses of J/ψ and

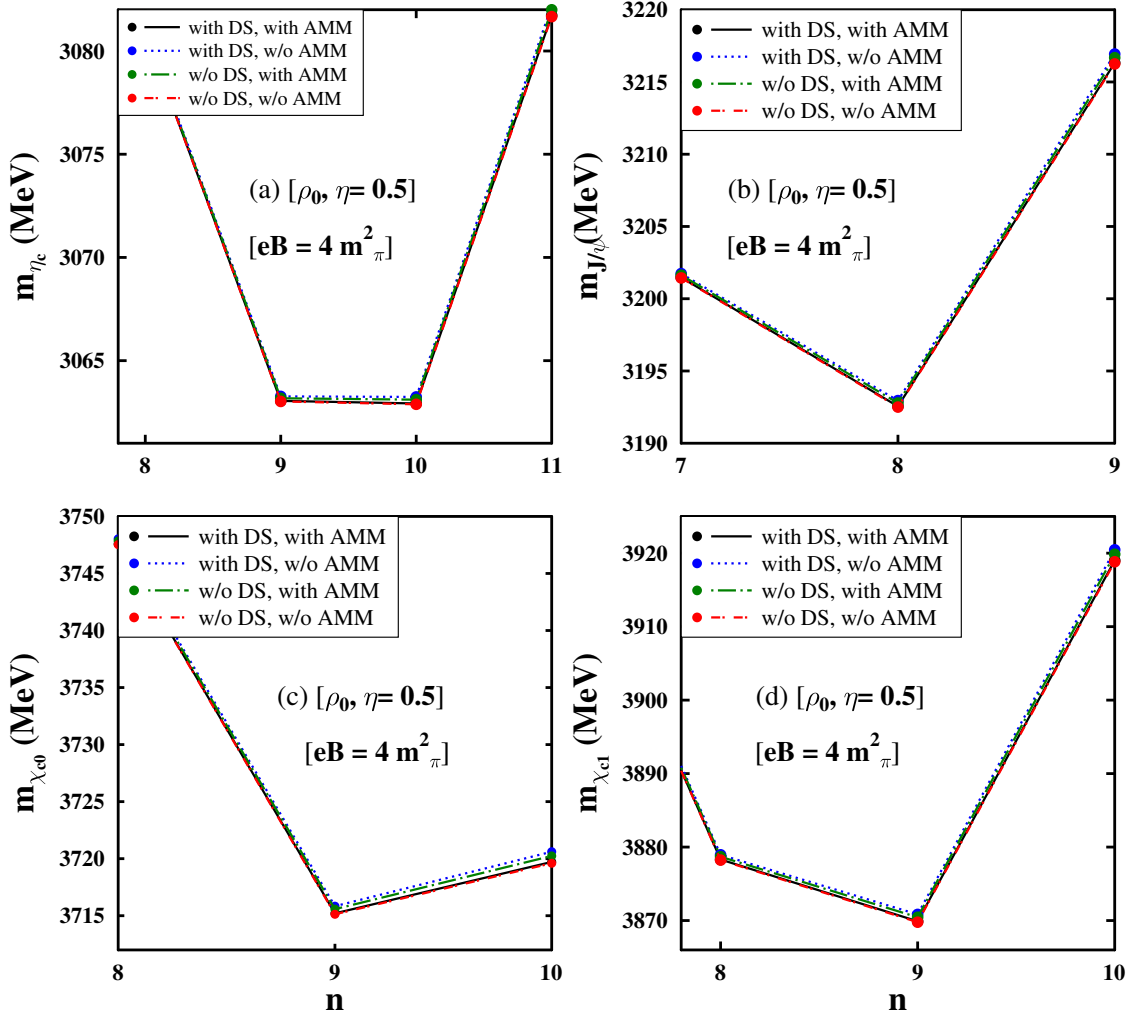


FIG. 4: Masses (MeV) are plotted as functions of n , for J/ψ , η_c , χ_{c0} and χ_{c1} , at $\rho_B = \rho_0$, $\eta = 0.5$. Contributions of the Dirac sea (DS), Landau quantization of protons, and nucleons AMMs, at $eB = 4m_\pi^2$, are considered. Comparison are made when effects of DS and nucleons AMMs, are not taken into account.

η_c are found to be 3196.56 MeV and 3066.57 MeV, respectively. The values of the twist-2 condensate, G_2 is zero, and of $\langle \frac{\alpha_s}{\pi} G_{\mu\nu}^a G^{a\mu\nu} \rangle$ is $(373.02 \text{ MeV})^4$ at vacuum. The vacuum masses of χ_{c0} and χ_{c1} are obtained as 3720.95 MeV and 3878.55 MeV, respectively. For any particular state (i) of heavy quarkonia, the quantity m_i^* , in equation (9), in terms of the ratio of two consecutive moments and parameters involving the renormalization scale, ξ , can be varied as a function of n . The minimum value of m_i^* corresponds to the physical mass of the state. For large values of n , the contributions of the higher lying resonances

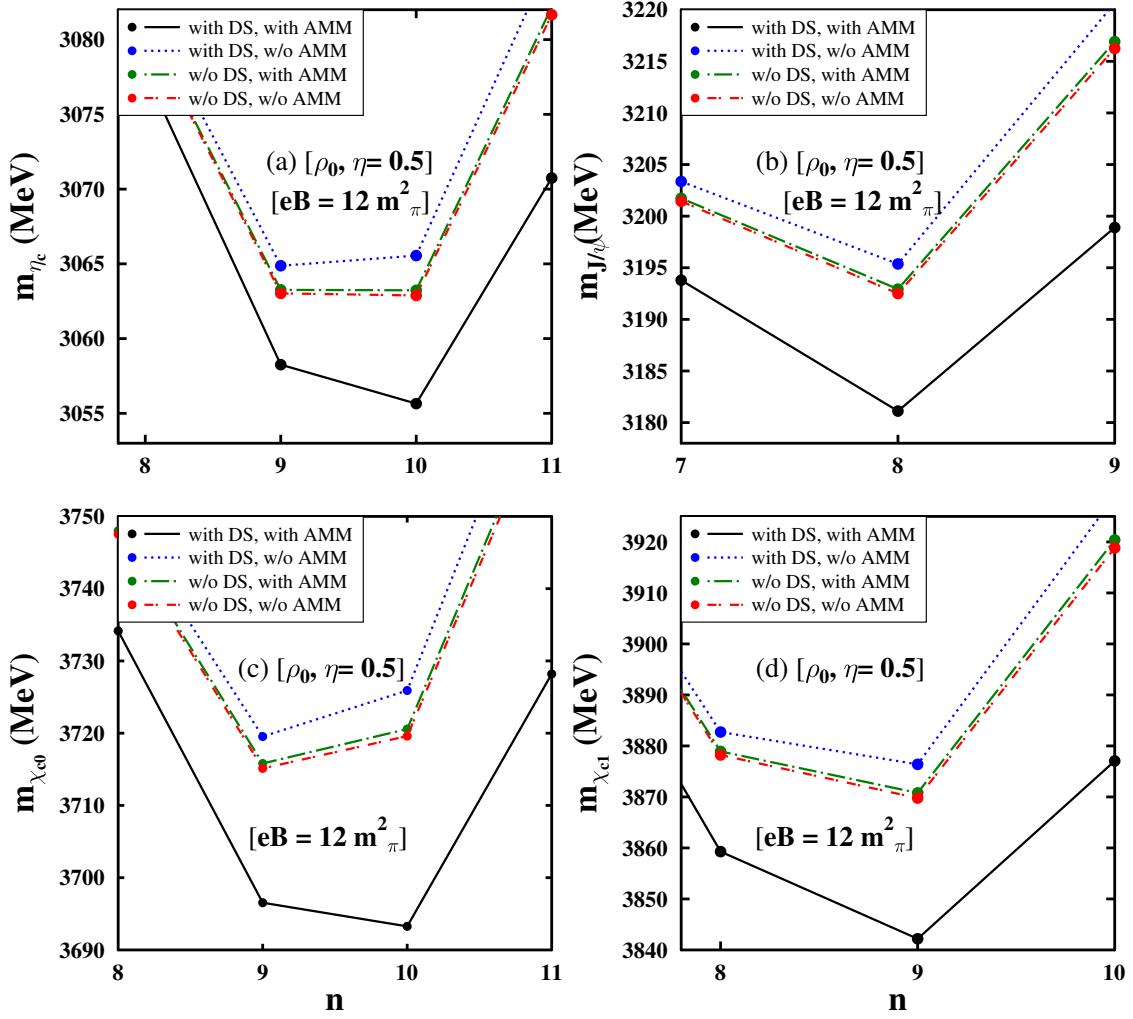


FIG. 5: Masses (MeV) are plotted as functions of n , for J/ψ , η_c , χ_{c0} and χ_{c1} at $\rho_B = \rho_0$, $\eta = 0.5$. Contributions of the Dirac sea (DS), Landau quantization of protons, and nucleons AMMs, at $eB = 12m_\pi^2$, are considered. Comparison are made when effects of DS and nucleons AMMs, are not taken into account.

and continuum states can be neglected. On the other hand, it considers the contribution of the higher dimensional operators in the OPE side, which do not let the first order perturbation theory to hold. To minimize the contributions of the higher dimensional operators, the value of Q_0^2 and hence of ξ must be chosen nonzero. For a certain value of ξ , a range of values of n is obtained, which correspond to the lowest lying resonance in the phenomenological side, and the OPE side becomes valid [75]. The stability region in n changes with ξ . Breakdown occurs in the stability region for small values of n due to the contribution

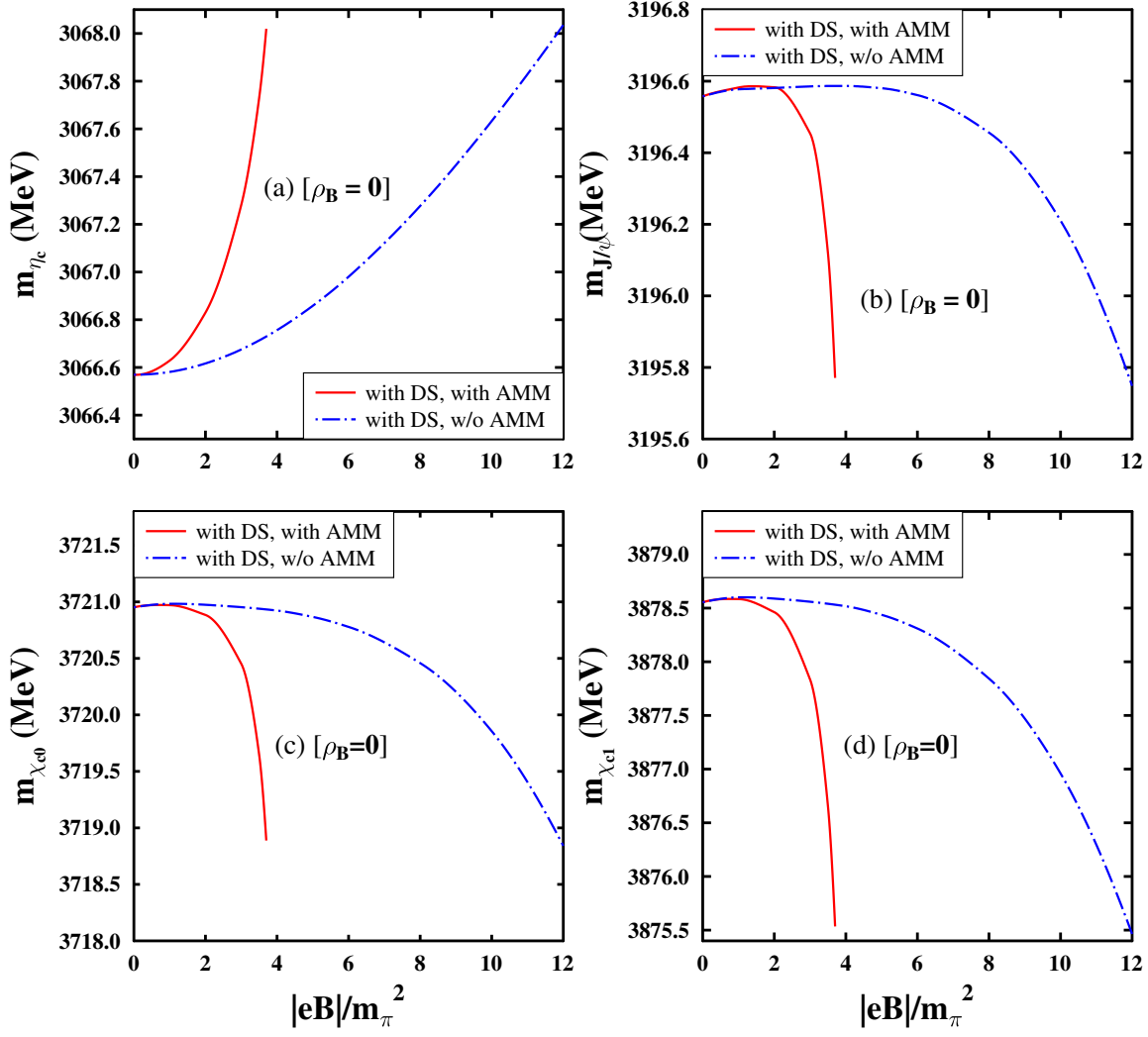


FIG. 6: Masses (in MeV) as functions of $|eB|$ (in units of m_π^2) are plotted for J/ψ , η_c , χ_{c0} and χ_{c1} states of charmonia, at $\rho_B = 0$. The contribution of Dirac sea (DS), along with the AMMs of nucleons, are considered at $\rho_B = 0$.

of the higher lying resonances. At large values of n the perturbation theory breaks down. In our calculations, the stability range in n , for the $1S$ and $1P$ states of charmonium and bottomonium are in accordance with the original works of [74, 75]. The physical mass of the vector state, J/ψ is obtained at $n = 8$ for $\xi = 1$. The range is set to magnify the position of the minimum value of m_i^* . In order to find the masses of η_c , J/ψ , χ_{c0} and χ_{c1} charmonium states, their corresponding m_i^* as calculated from equation (9) are plotted as functions of n , in Fig.[1] for $\rho_B = 0$ and $|eB| = 0, 2m_\pi^2$ and in Figs.[2]-[5] for $\rho_0, \eta = 0, 0.5$ and $|eB| = 4m_\pi^2$ and $12m_\pi^2$. At zero density and finite magnetic field, the effect is through

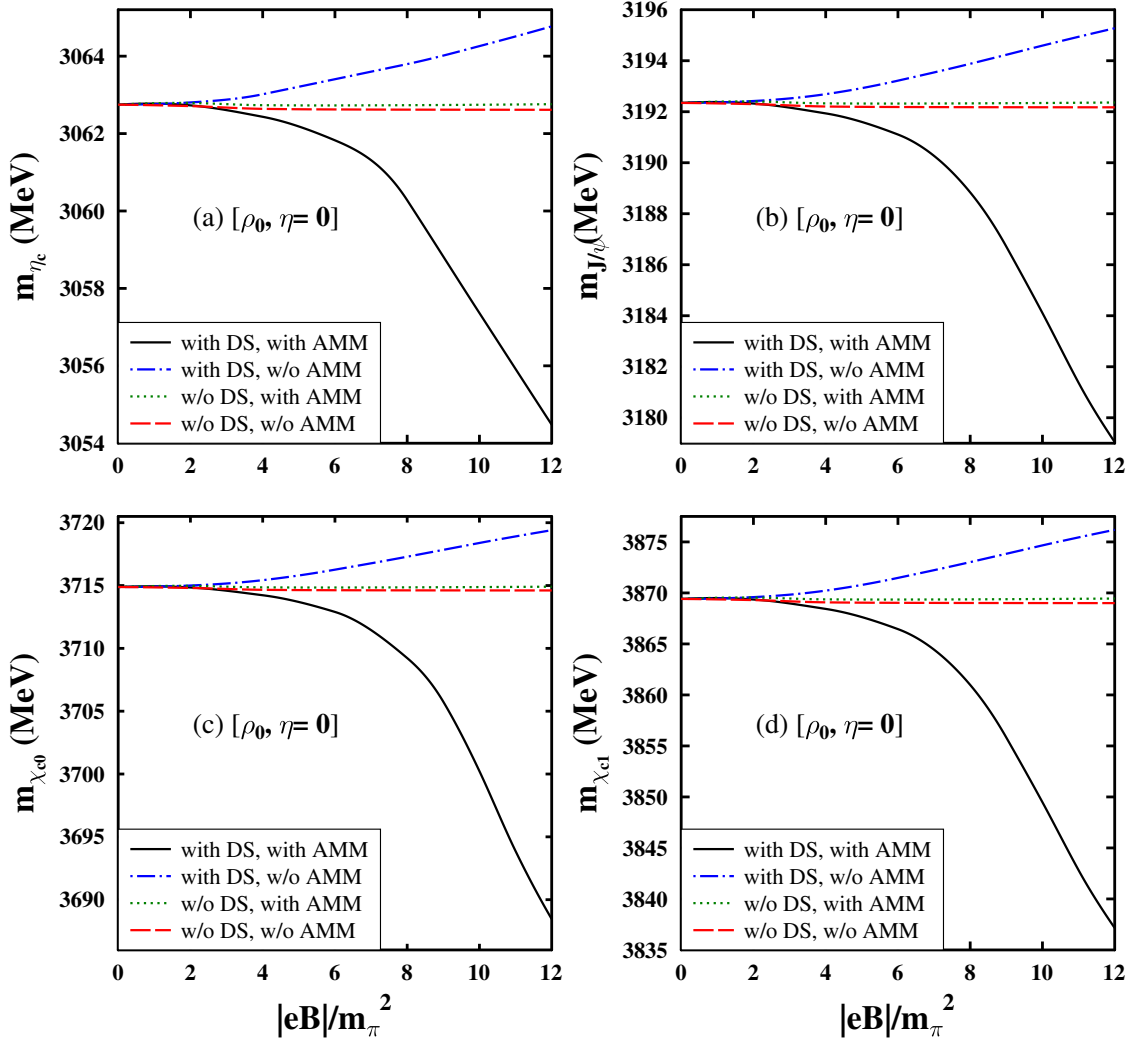


FIG. 7: Masses of J/ψ , η_c , χ_{c0} and χ_{c1} states of charmonium (in MeV) are plotted as functions of $|eB|/m_\pi^2$, at ρ_0 and $\eta = 0$. The masses with Dirac sea (DS) contribution (solid line with AMM and dot-dashed line without AMM) are compared to the case when only Landau level contribution is there (dotted line with AMM and long-dashed line without AMM).

the magnetized Dirac sea only, no Landau level contribution is there in the absence of matter part. The masses are calculated by considering the nonzero anomalous magnetic moments (AMMs) of the nucleons and compared to the case when AMM is zero. The scalar fields are solved with and without the magnetized Dirac sea contribution at finite magnetic field along with the Landau level contribution of protons and the non zero anomalous magnetic moments (AMM) of the nucleons at finite density matter. The values of the scalar gluon condensate, in terms of the scalar dilaton field, χ and the scalar fields σ , ζ (in the limit of

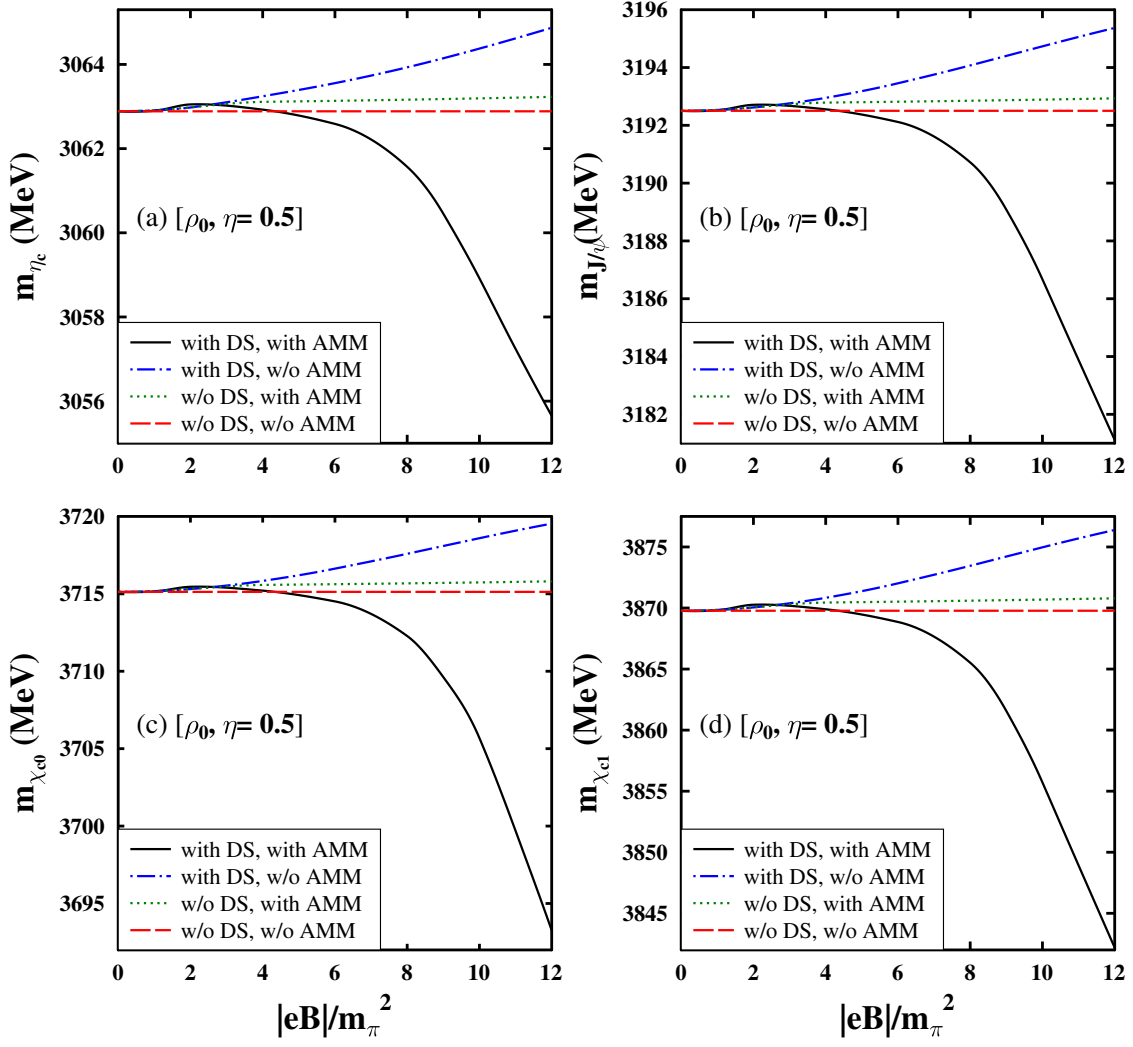


FIG. 8: Masses of J/ψ , η_c , χ_{c0} and χ_{c1} states of charmonium (in MeV) are plotted as functions of $|eB|/m_\pi^2$, at ρ_0 and $\eta = 0.5$. The masses with Dirac sea (DS) effects are compared to the case when only Landau level contribution is there.

finite quark masses), are (in $(\text{MeV})^4$), $\langle \frac{\alpha_s}{\pi} G_{\mu\nu}^a G^{a\mu\nu} \rangle = (373)^4$, $(372.88)^4$, $(372.48)^4$, $(371.44)^4$ and $(370.36)^4$ at $|eB|/m_\pi^2 = 1, 2, 3, 3.7$ and 3.9 , respectively for $\rho_B = 0$ and with AMM case. For the case of without AMM, at zero density, values of $\langle \frac{\alpha_s}{\pi} G_{\mu\nu}^a G^{a\mu\nu} \rangle$ are $(373.01 \text{ MeV})^4$, $(372.93 \text{ MeV})^4$, $(372.49 \text{ MeV})^4$ and $(371.41 \text{ MeV})^4$ at $|eB|/m_\pi^2 = 2, 4, 8$ and 12 , respectively. The expectation value of the twist-2 gluon condensate, G_2 becomes non-zero at vacuum and in presence of an external magnetic field, due to the Dirac sea contribution. Thus, the values of G_2 in terms of the scalar fields [from equation (7)] are given as $(57.26 \text{ MeV})^4$ (for $1S$ states), $(56.19 \text{ MeV})^4$ (for $1P$ states) at $2m_\pi^2$, and $(92.31 \text{ MeV})^4$ (for

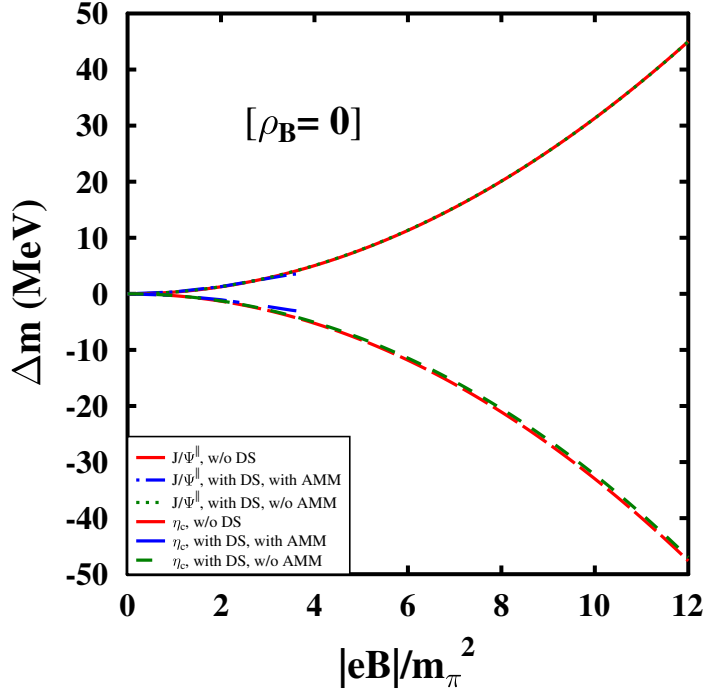


FIG. 9: Mass shifts (in MeV) are plotted as functions of $|eB|$ (in units of m_π^2), by considering the spin-mixing between the longitudinal component of J/ψ and η_c states of S -wave charmonium. Mixing effects are calculated with and without the magnetized Dirac sea (DS) contribution, and nucleons AMMs at $\rho_B = 0$.

$1S$), $(90.59 \text{ MeV})^4$ (for $1P$) at $3.7m_\pi^2$, with nonzero AMMs of nucleons. In the case of zero AMM, zero density, the values are $(35.99 \text{ MeV})^4$ (for $1S$), $(35.32 \text{ MeV})^4$ (for $1P$) at $2m_\pi^2$, and $(74.94 \text{ MeV})^4$ (for $1S$), $(73.55 \text{ MeV})^4$ (for $1P$) at $8m_\pi^2$. The running coupling constant, α_s is a function of the renormalization scale, ξ , thus different choices of ξ for the S -wave and P -wave states lead to slight variation in G_2 values. The values of these condensates are seen to change considerably with the magnetic field, at zero density, accounting for the Dirac sea effect, whereas there is no effect from the Landau quantization of protons. The variation in masses as a function of magnetic field thus obtained from the modified gluon condensates, are shown in Fig.[6] for $\rho_B = 0$, and in Figs.[7]-[8] for $\rho_0, \eta = 0, 0.5$, for the $1S$ ($J/\psi, \eta_c$) and $1P$ (χ_{c0}, χ_{c1}) states of charmonium. At finite density matter, $\rho_B = \rho_0$, the contribution from the protons Landau energy levels and anomalous magnetic moments

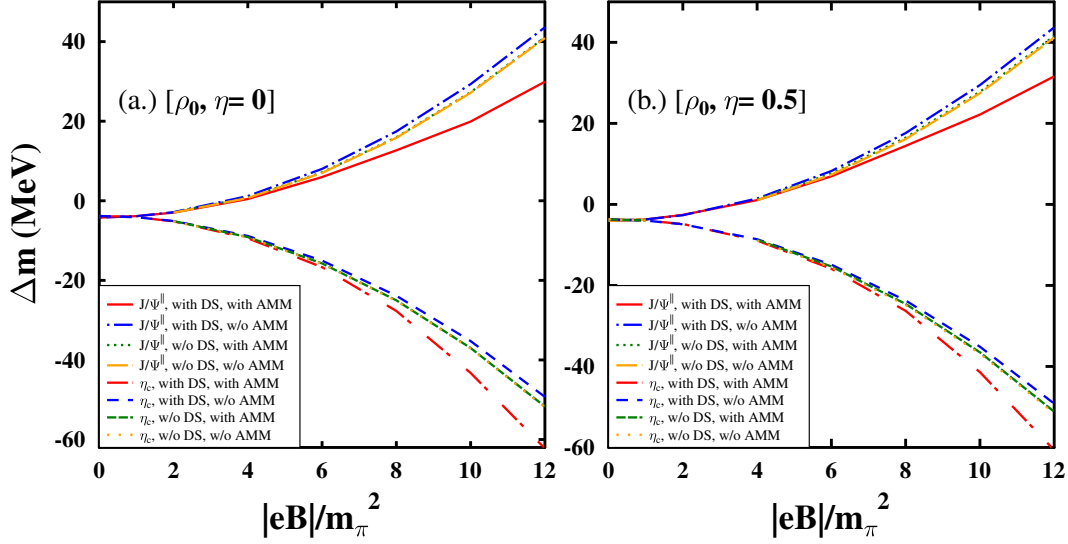


FIG. 10: Mass shifts (in MeV) are plotted as functions of $|eB|/m_\pi^2$, accounting the effects of mixing between J/ψ^\parallel - η_c states. Mixing effects are calculated with and without the Dirac sea (DS) contribution at $\rho_B = \rho_0$. Plot (a.) for symmetric ($\eta = 0$) and plot (b.) for asymmetric ($\eta = 0.5$) nuclear matter.

of nucleons are taken into account together with the Dirac sea effects through the scalar densities of protons and neutrons. In Figs.[7]-[8], masses are compared with the case when there is no Dirac sea effect. The in-medium masses of the J/ψ , η_c , χ_{c0} , and χ_{c1} states of charmonium decrease (increase) with increasing magnetic field, accounting for the Dirac sea contribution, for the case of nonzero AMMs (zero AMM) of nucleons. In comparison to such effects, there are almost no change observed with increasing magnetic field, accounting for only the protons Landau energy levels in nuclear matter. The observed behavior imply that, an important effect due to the nonzero anomalous magnetic moments of nucleons is coming through the Dirac sea contribution. The values of the QCD gluon condensates, $\langle \frac{\alpha_s}{\pi} G_{\mu\nu}^a G^{a\mu\nu} \rangle$ and G_2 (for $1S$ and $1P$ states) at $\rho_0, \eta = 0$ and with AMM, are given respectively, as: $(371.78 \text{ MeV})^4, -9.7576 \times 10^7 \text{ MeV}^4$ ($1S$), $-9.0513 \times 10^7 \text{ MeV}^4$ ($1P$) at $2m_\pi^2$; $(371.58 \text{ MeV})^4, -1.0083 \times 10^8 \text{ MeV}^4$ ($1S$), $-9.3531 \times 10^7 \text{ MeV}^4$ ($1P$) at $4m_\pi^2$; and $(369.87 \text{ MeV})^4, -1.1937 \times 10^8 \text{ MeV}^4$ ($1S$), $-1.1073 \times 10^8 \text{ MeV}^4$ ($1P$) at $8m_\pi^2$; which for the case of without AMM are: $(371.83 \text{ MeV})^4, -9.6866 \times 10^7 \text{ MeV}^4$ ($1S$), $-8.9855 \times 10^7 \text{ MeV}^4$ ($1P$) at

$2m_\pi^2$; $(371.9643 \text{ MeV})^4$, $-9.4449 \times 10^7 \text{ MeV}^4$ ($1S$), $-8.7613 \times 10^7 \text{ MeV}^4$ ($1P$) at $4m_\pi^2$; and $(372.5342 \text{ MeV})^4$, $-8.1640 \times 10^7 \text{ MeV}^4$ ($1S$), $-7.5731 \times 10^7 \text{ MeV}^4$ ($1P$) at $8m_\pi^2$. The condensates in the asymmetric nuclear matter ($\eta = 0.5$), at the nuclear matter saturation density (ρ_0) are given respectively by: $(371.97 \text{ MeV})^4$, $-9.3679 \times 10^7 \text{ MeV}^4$ ($1S$), $-8.6899 \times 10^7 \text{ MeV}^4$ ($1P$) at $2m_\pi^2$; $(371.89 \text{ MeV})^4$, $-9.5119 \times 10^7 \text{ MeV}^4$ ($1S$), $-8.8234 \times 10^7 \text{ MeV}^4$ ($1P$) at $4m_\pi^2$; and $(370.91 \text{ MeV})^4$, $-1.0893 \times 10^8 \text{ MeV}^4$ ($1S$), $-1.0104 \times 10^8 \text{ MeV}^4$ ($1P$) at $8m_\pi^2$, for the case of nonzero AMM. The values in case of without AMM are: $(371.92 \text{ MeV})^4$, $-9.4527 \times 10^7 \text{ MeV}^4$ ($1S$), $-8.7685 \times 10^7 \text{ MeV}^4$ ($1P$) at $2m_\pi^2$; $(372.08 \text{ MeV})^4$, $-9.1366 \times 10^7 \text{ MeV}^4$ ($1S$), $-8.4753 \times 10^7 \text{ MeV}^4$ ($1P$) at $4m_\pi^2$; and $(372.61 \text{ MeV})^4$, $-7.8478 \times 10^7 \text{ MeV}^4$ ($1S$), $-7.2798 \times 10^7 \text{ MeV}^4$ ($1P$) at $8m_\pi^2$, for $\langle \frac{\alpha_s}{\pi} G_{\mu\nu}^a G^{a\mu\nu} \rangle$ and G_2 of $1S$ and $1P$ states, respectively. The masses plotted incorporating the effects of magnetized Dirac sea, are denoted as "with DS, with AMM" when the anomalous magnetic moments of the nucleons are considered and "with DS, w/o AMM" when not considered. The different behavior of the pseudoscalar meson mass with magnetic field in the absence of nuclear matter, can be attributed to the variation in the Wilson coefficients for different channels.

The mixing between the longitudinal component of the vector meson, J/ψ^{\parallel} and the pseudoscalar meson, η_c is also studied in the present work using a phenomenological Lagrangian approach. The parameter $g_{PV} \equiv g_{\eta_c J/\psi}$ is evaluated to be 2.094 from the observed radiative decay width, $\Gamma(J/\psi \rightarrow \eta_c \gamma)$ in vacuum of 92.9 keV [76], using equation (18). This effect gives rise to increasing (decreasing) mass of the J/ψ^{\parallel} (η_c) with magnetic field. In Figs.[9]-[10], mass shifts of the J/ψ^{\parallel} and η_c are plotted as a function of $|eB|/m_\pi^2$ at $\rho_B = 0$ and $\rho_B = \rho_0$, $\eta = 0, 0.5$, incorporating the PV mixing effect in the magnetic field background, by taking into account the additional contribution of magnetized Dirac sea.

B. Bottomonium states

In this section, the results for the in-medium masses of the bottomonium ground states, namely the $1S$ -wave: $\Upsilon(1S)$ (3S_1), η_b (1S_0) and $1P$ -wave: χ_{b0} (3P_0), χ_{b1} (3P_1), are illustrated in the magnetized, asymmetric nuclear matter with the additional contribution from the magnetized Dirac sea. The masses are calculated using the QCD sum rule approach in a similar fashion as described above for the corresponding $1S$ and $1P$ states of charmonium. The running bottom quark mass, $m_b(\xi)$ and the running coupling constant, $\alpha_s(\xi)$, as given

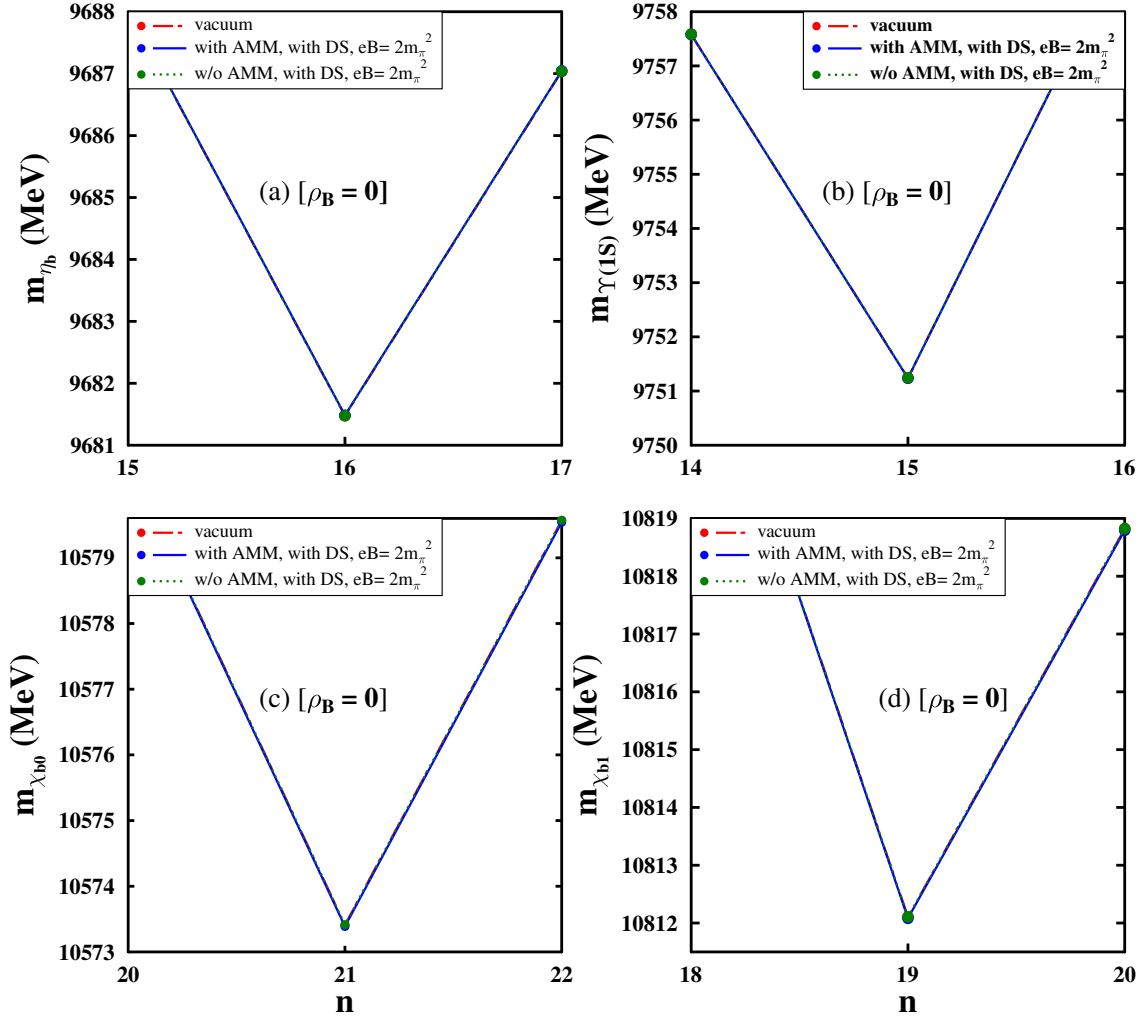


FIG. 11: Masses (in MeV) of $1S$ ($\Upsilon(1S)$, η_b) and $1P$ (χ_{b0} , χ_{b1}) states of bottomonium are plotted as functions of n , at $\rho_B = 0$, considering Dirac sea (DS) effects at $eB = 2m_\pi^2$, with and without nucleons AMMs.

by equations (15) and (16) respectively, are different from the charmonium states, as the number of current quark flavors, $n_f = 5$ for bottom quark, which was $n_f = 4$ for the charm quark, also the ξ -independent parameters of the quark mass and couplings (in equations (15) and (16), respectively) are different in the two sectors of charm and bottom quarks. The scalar gluon condensate, $\langle \frac{\alpha_s}{\pi} G_{\mu\nu}^a G^{a\mu\nu} \rangle$ through the ϕ_b term and the twist-2 gluon condensate, G_2 in ϕ_c term, again incorporate the effects of density, magnetic fields and isospin asymmetry of the nuclear medium on the bottomonium masses. In the present investigation, we have studied the additional contribution of magnetized Dirac sea on the bottomonium masses.

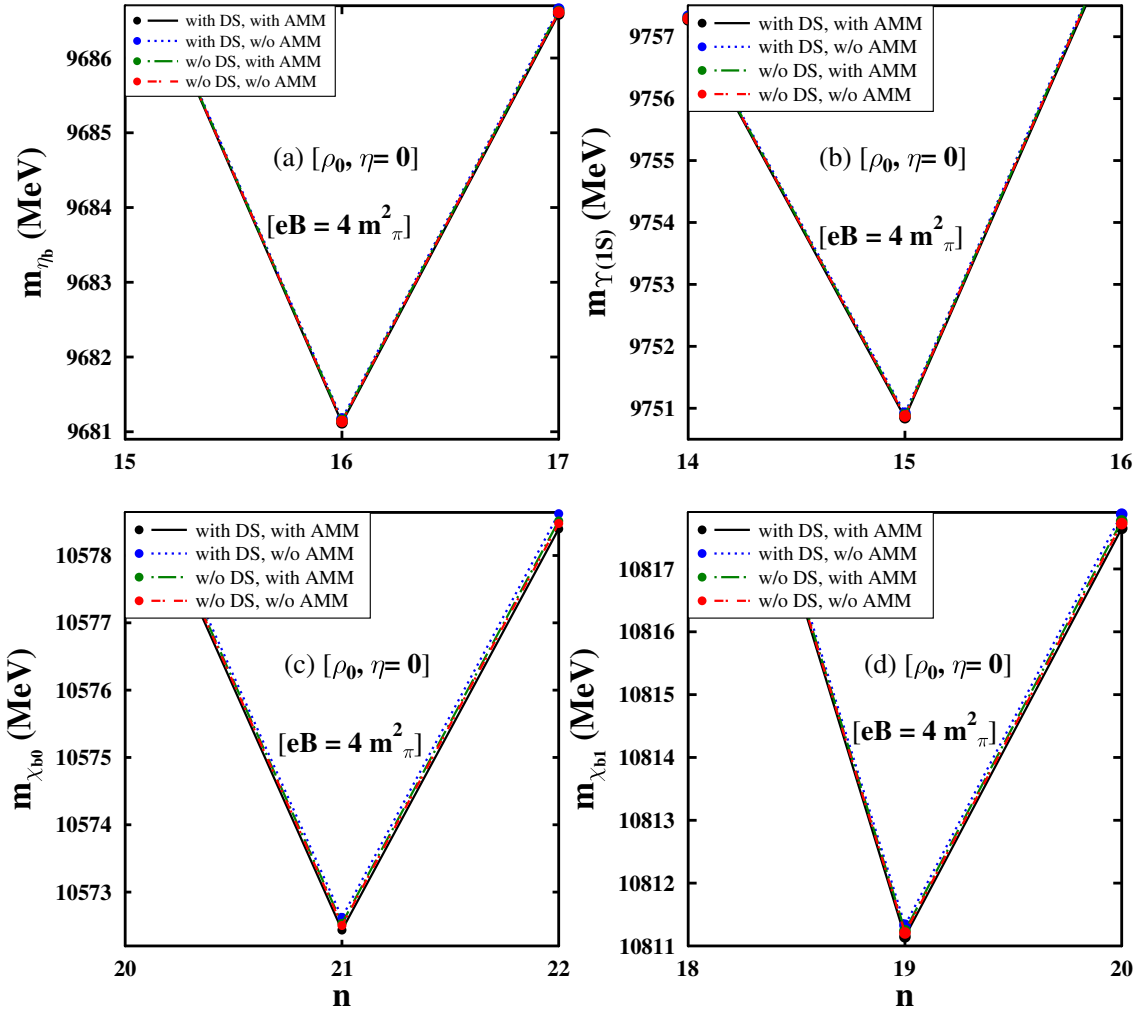


FIG. 12: Masses (MeV) are plotted as functions of n , for $\Upsilon(1S)$, η_b , χ_{b0} and χ_{b1} states at $\rho_B = \rho_0$, $\eta = 0$. Effects of Dirac sea, Landau level contributions of protons, and AMMs of nucleons, at $eB = 4m_\pi^2$ are considered.

The scalar densities of protons (ρ_p^s) and neutrons (ρ_n^s) have contributions from the Dirac sea, in addition to the Landau level contributions of protons in the Fermi sea of nucleons. The values of the scalar gluon condensate, $\langle \frac{\alpha_s}{\pi} G_{\mu\nu}^a G^{a\mu\nu} \rangle$ remain same (as can be inferred from equation (8)) with what have already discussed, for $\rho_B = 0$ as well as ρ_0 , and for different values of magnetic fields. However, the values of twist-2 gluon condensates, from equation (7), depend on α_s , which lead to different values for G_2 of $1S$ and $1P$ states of bottomonium. For e.g., at $\rho_B = 0$, with AMM case, these are $(51.83 \text{ MeV})^4$ (for $1S$), and $(51.23 \text{ MeV})^4$ (for $1P$) at $|eB| = 2m_\pi^2$, which are different to that in the charmonium sector $[(57.26 \text{ MeV})^4$

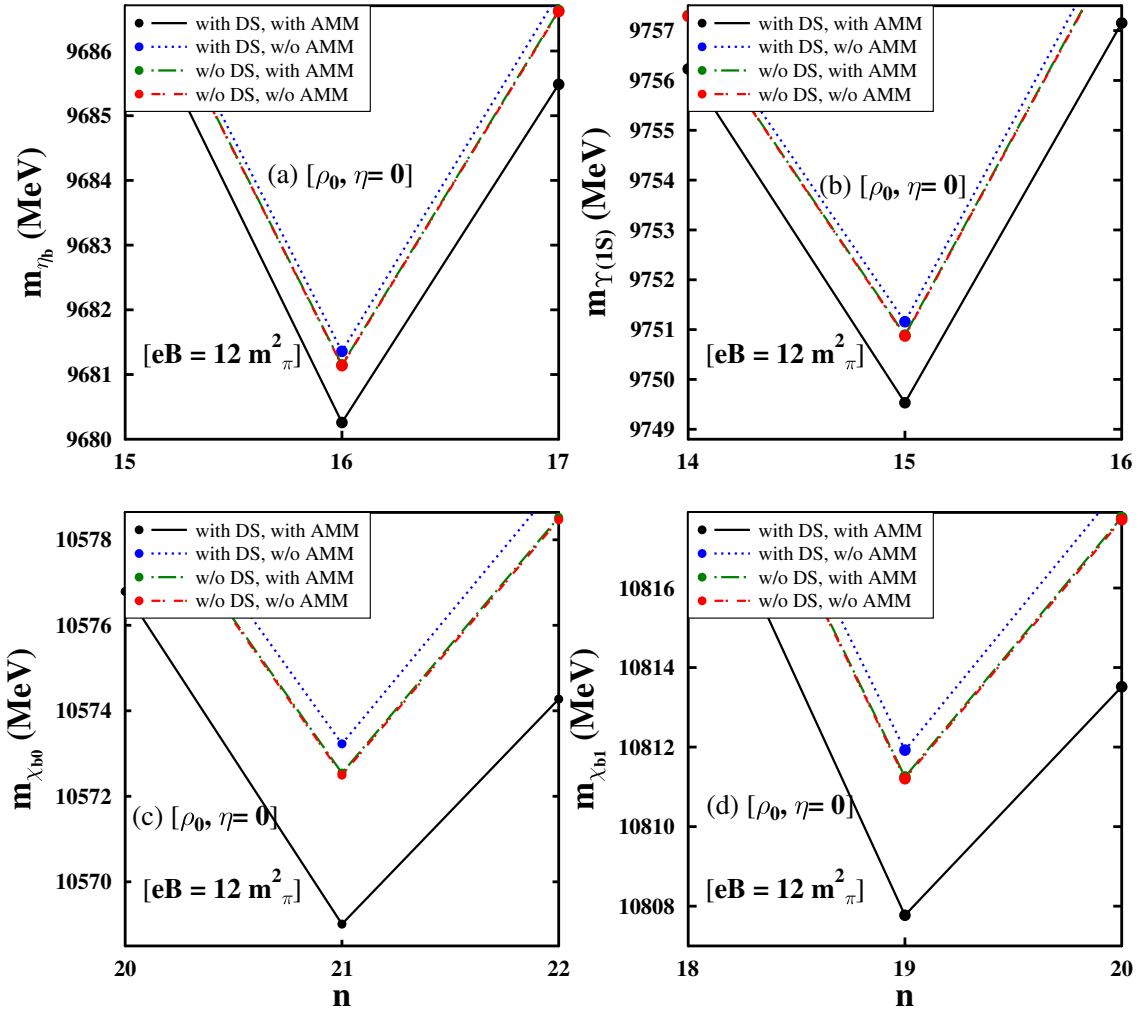


FIG. 13: Masses (MeV) are plotted as functions of n , for $\Upsilon(1S)$, η_b , χ_{b0} and χ_{b1} states at $\rho_B = \rho_0$, $\eta = 0$. Effects of Dirac sea and Landau level contributions of protons, at $eB = 12m_\pi^2$ are considered.

(for $1S$), and $(56.19 \text{ MeV})^4$ (for $1P$) at $|eB| = 2m_\pi^2$, but the variation in the values with increasing magnetic field are found to be similar in both sectors. Therefore, using the values of ϕ_b and ϕ_c , the in-medium masses of the bottomonium ground states are calculated using equation (9). In presence of an external magnetic field, the spin-magnetic field interaction are studied for the $1S$ states of bottomonium using a Hamiltonian approach. The effective masses of $\Upsilon^{\parallel}(1S)$ and η_b , taking into account the spin-mixing effect, are computed using Eq. (21).

Similar to the charmonium sector, the value of the renormalization scale, $\xi = 1$ is chosen for the S -wave states and $\xi = 2.5$ is taken for the P -wave states to study their respective

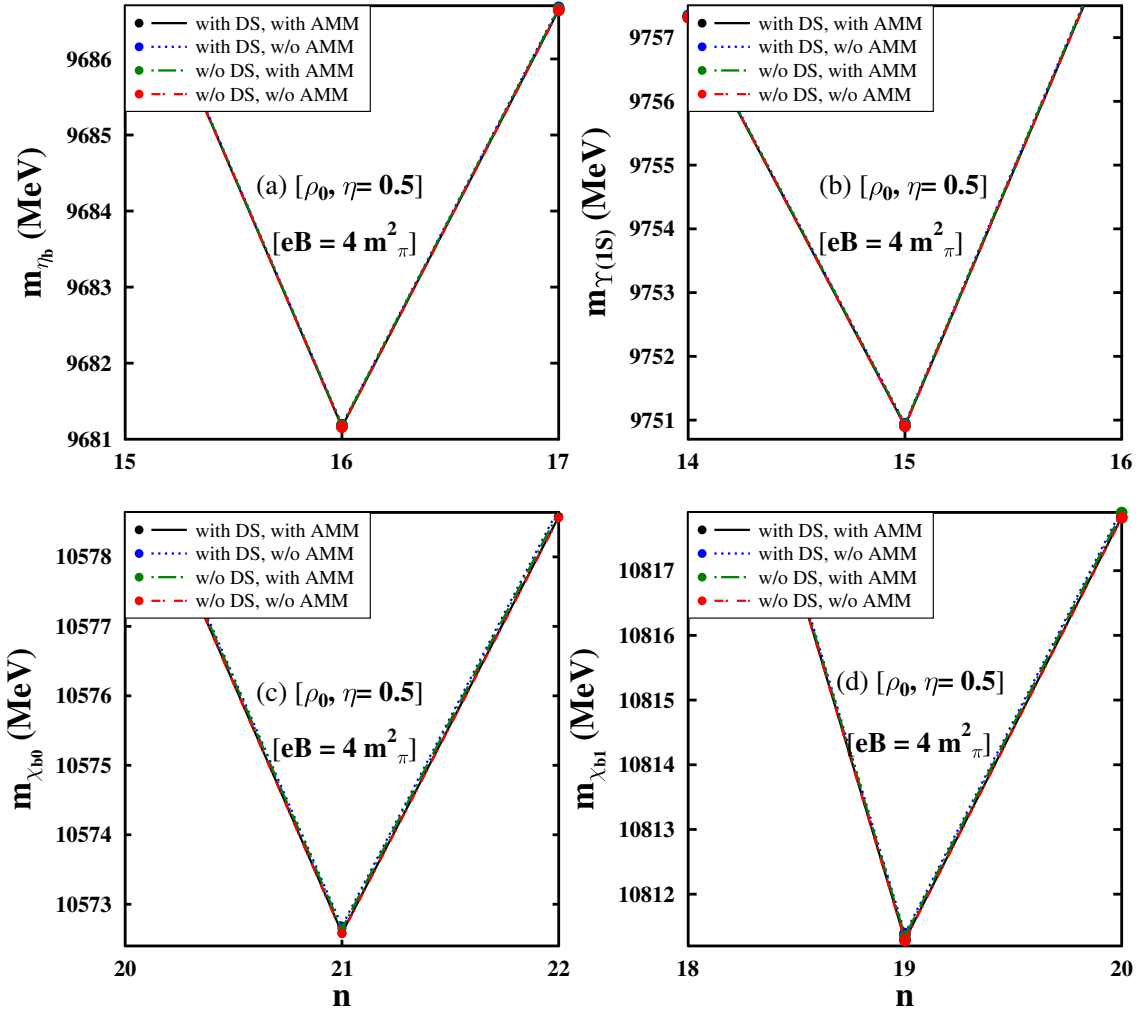


FIG. 14: Masses (MeV) are plotted as functions of n , for $\Upsilon(1S)$, η_b , χ_{b0} and χ_{b1} states at $\rho_B = \rho_0$, $\eta = 0.5$. Dirac sea effects and protons Landau level contributions, at $eB = 4m_\pi^2$ are considered.

in-medium masses. These choices lead to the ξ -dependent running coupling constant and running bottom quark mass, $\alpha_s = 0.1411$ and $m_b = 4.18$ GeV for the $1S$ states and $\alpha_s = 0.1346$ and $m_b = 4.13$ GeV for the $1P$ states of bottomonium, respectively. From these parameters and with ϕ_b calculated within the chiral effective model, the vacuum masses (in MeV) of $\Upsilon(1S)$ and η_b are obtained to be 9751.24 and 9681.47 respectively. The vacuum masses (in MeV) of χ_{b0} and χ_{b1} are obtained as 10573.41 and 10812.1, respectively. In Fig.11, masses of all the four bottomonium ground states ($\Upsilon(1S)$, η_b , χ_{b0} and χ_{b1}), are plotted as a function of the order of the moment, n . The value of n , corresponding to the minimum point gives the physical mass of the associated state. In this work, the masses plotted incorporating

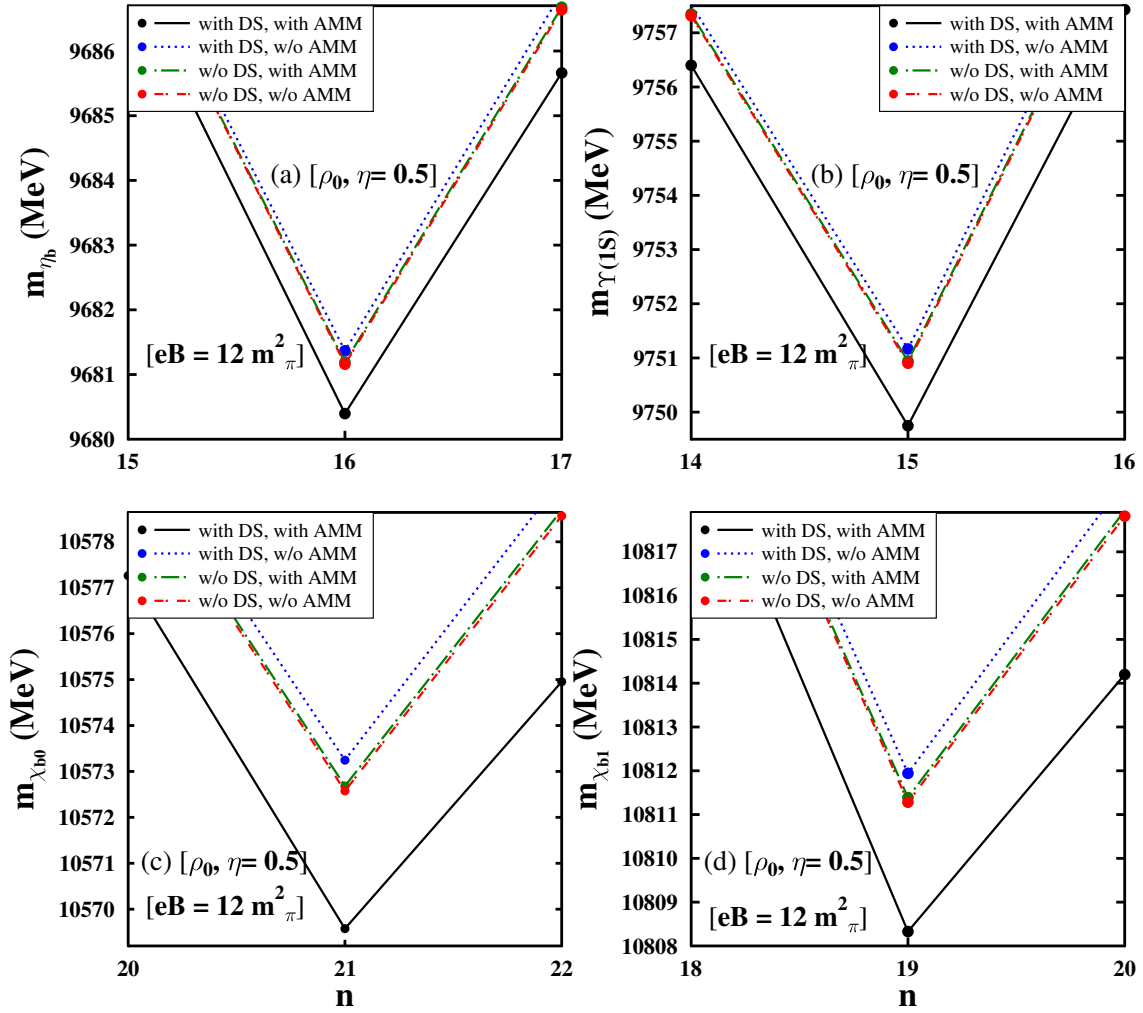


FIG. 15: Masses (MeV) are plotted as functions of n , for $\Upsilon(1S)$, η_b , χ_{b0} and χ_{b1} states at $\rho_B = \rho_0$, $\eta = 0.5$. Dirac sea effects and protons Landau level contributions, at $eB = 12m_\pi^2$ are considered.

the effects of magnetized Dirac sea (DS), are denoted as "with DS, with AMM" when the anomalous magnetic moments of the nucleons are considered and "with DS, w/o AMM" when AMM is taken to be zero. In Figs.[12]-[15], the in-medium masses of the $1S$ -wave and $1P$ -wave states are plotted as functions of n , at ρ_0 , for symmetric ($\eta = 0$) as well as asymmetric ($\eta = 0.5$) nuclear matter, and at magnetic field values of $|eB|/m_\pi^2 = 4, 12$. As can be seen from Fig.13 and Fig.15, the anomalous magnetic moments of the nucleons have distinguishable contribution on the masses at high magnetic field, in the case of DS effect as compared to the "w/o DS" case (when there is no Dirac sea contribution). In order to see the importance of the Dirac sea effect on the bottomonium masses, Figs.[17]-[18] illustrate the

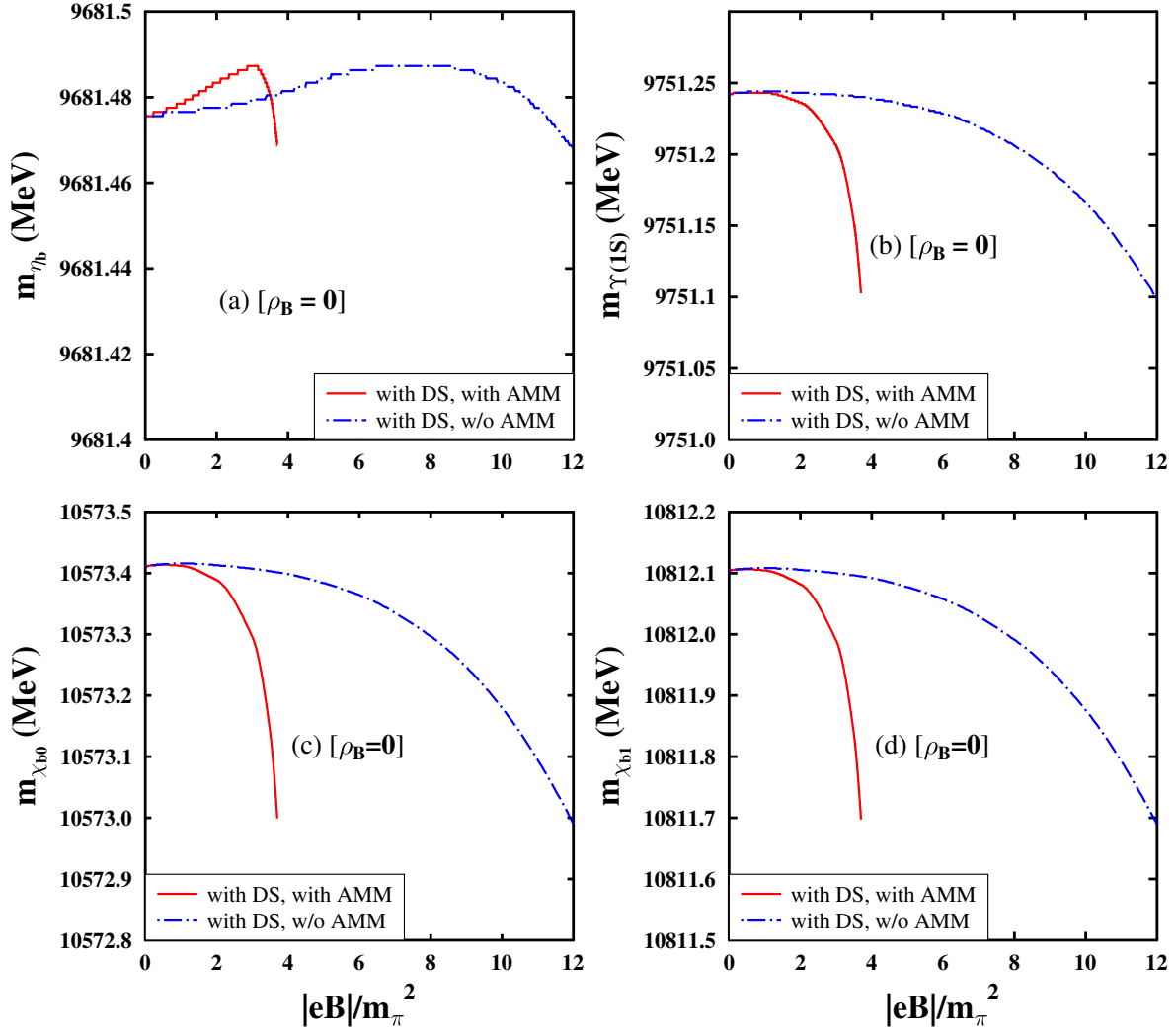


FIG. 16: Masses (in MeV) are plotted as function of $|eB|/m_\pi^2$, for $\Upsilon(1S)$, η_b , χ_{b0} and χ_{b1} states of bottomonium, at $\rho_B = 0$. Contributions of DS and nucleons AMMs, are there in the vacuum.

variation of masses with magnetic field and compare the two situations, when the Dirac sea contribution is there along with the protons Landau quantization and when it is absent, at finite magnetic field. The masses of the four lowest states of bottomonium have appreciable modifications with rising magnetic field, as compared to the no-sea calculation. In Fig.16, the mass variation with magnetic field are shown for zero density, $\rho_B = 0$, and the behavior shown for $\Upsilon(1S)$, χ_{b0} and χ_{b0} indicate a lowering of their masses with magnetic field whereas that of η_b is seen to rise at first up to $eB = 8m_\pi^2$ (without AMM) then decrease. The masses are plotted up to $eB = 3.9m_\pi^2$ at $\rho_B = 0$, including the anomalous magnetic moments of the nucleons. Thus, the effect of anomalous magnetic moment on the bottomonium states

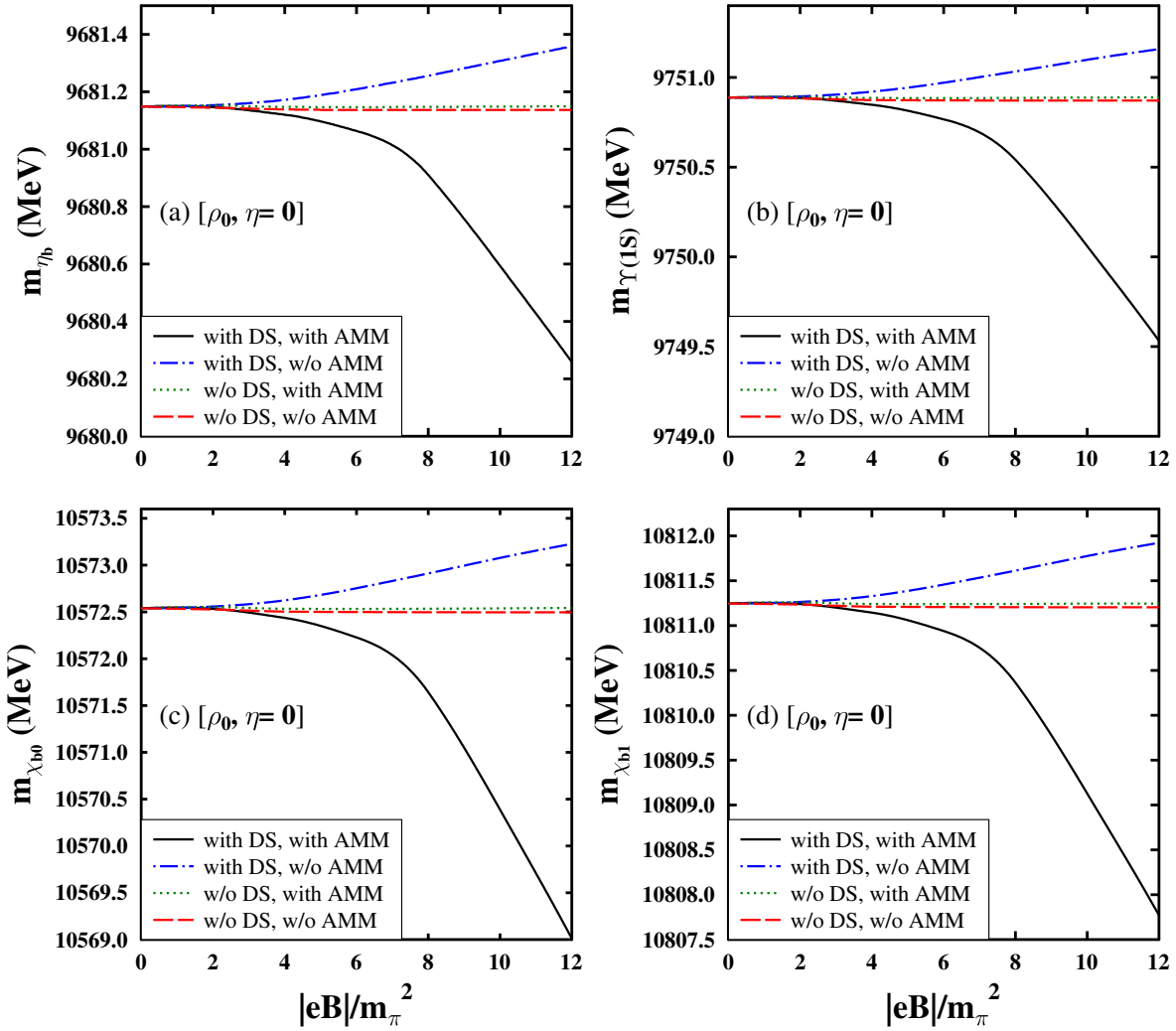


FIG. 17: Masses (in MeV) of $\Upsilon(1S)$, η_b , χ_{b0} and χ_{b1} states of bottomonium as functions of $|eB|/m_\pi^2$, at $\rho_B = \rho_0$, $\eta = 0$. The masses computed with Dirac sea (DS) contribution (solid line with AMM and dot-dashed line without AMM), are compared to the case when only Landau level contribution is there (dotted line with AMM and long-dashed line without AMM).

are observed to be quite significant at zero as well as at finite density matter, accounting for the Dirac sea contribution. The different behavior of the pseudoscalar meson mass with magnetic field in the absence of nuclear matter, can be attributed to the distinct values of the Wilson coefficients for different current channels. The effect of the spin-magnetic field interaction on the longitudinal component of vector meson, $\Upsilon(1S)$ and pseudoscalar meson, η_b is studied here, using a Hamiltonian approach [56]. The mass of the bottom quark is taken to be $m_b = 4.7$ GeV [56] in the bottom quark Bohr magneton, $\mu_b = \frac{e/3}{2m_b}$. This effect gives

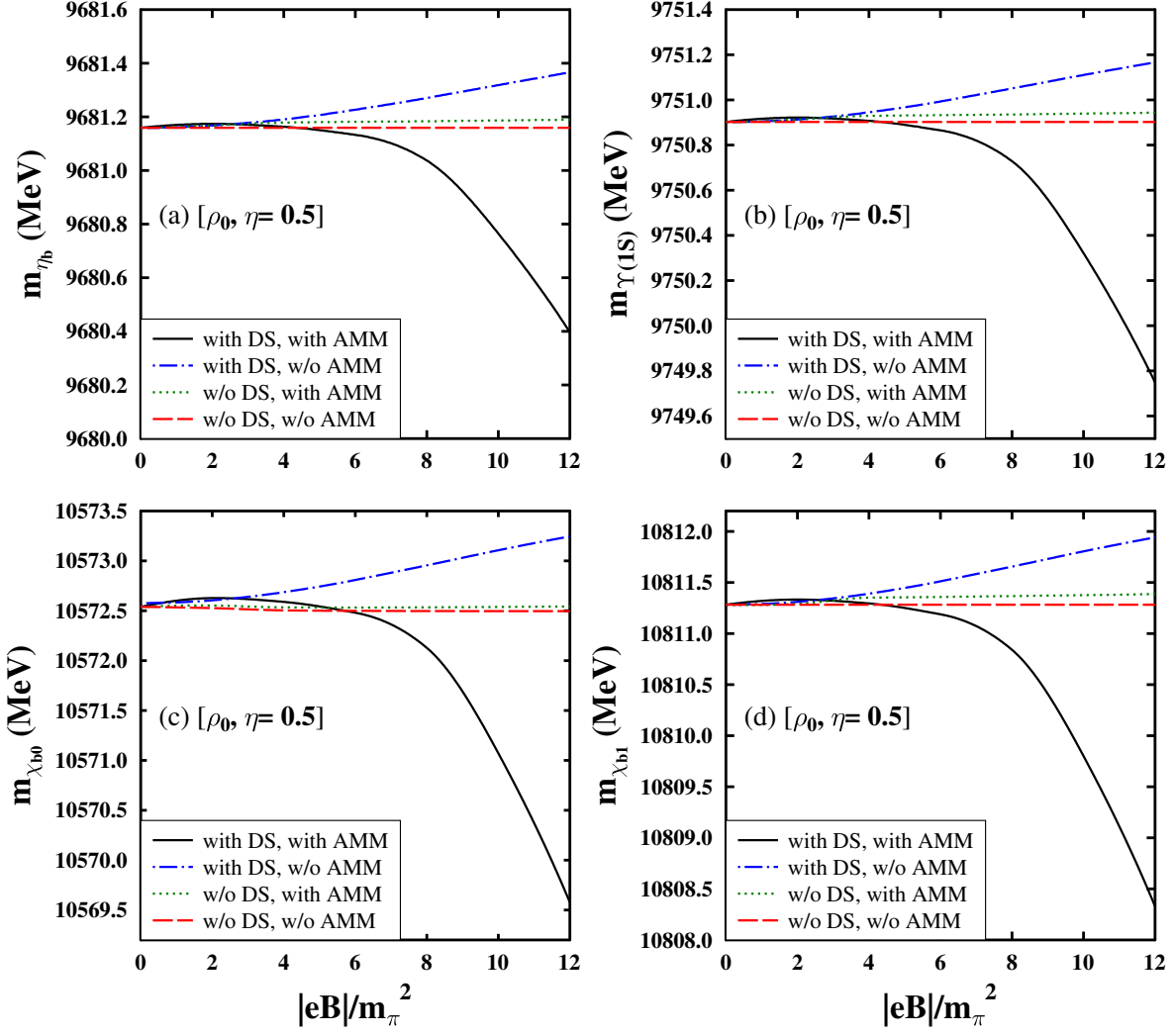


FIG. 18: Masses (in MeV) of $\Upsilon(1S)$, η_b , χ_{b0} and χ_{b1} states of bottomonium as functions of $|eB|/m_\pi^2$, at $\rho_B = \rho_0$, $\eta = 0.5$. The masses computed with the Dirac sea (DS) effects, are compared to the case when only Landau level contribution is there.

rise to increasing (decreasing) masses for the $\Upsilon^{\parallel}(1S)$ (η_b) states of S -wave bottomonium, with rising magnetic field. In Figs.[19]-[20], mass shifts of the $\Upsilon^{\parallel}(1S)$ and η_b are plotted as a function of $|eB|/m_\pi^2$ at $\rho_B = 0$, ρ_0 and $\eta = 0, 0.5$, accounting for the Dirac sea effect.

V. SUMMARY

In the summary, the in-medium masses of the $1S$ and $1P$ states of charmonium and bottomonium are studied using the QCD sum rule approach, in the magnetized nuclear medium,

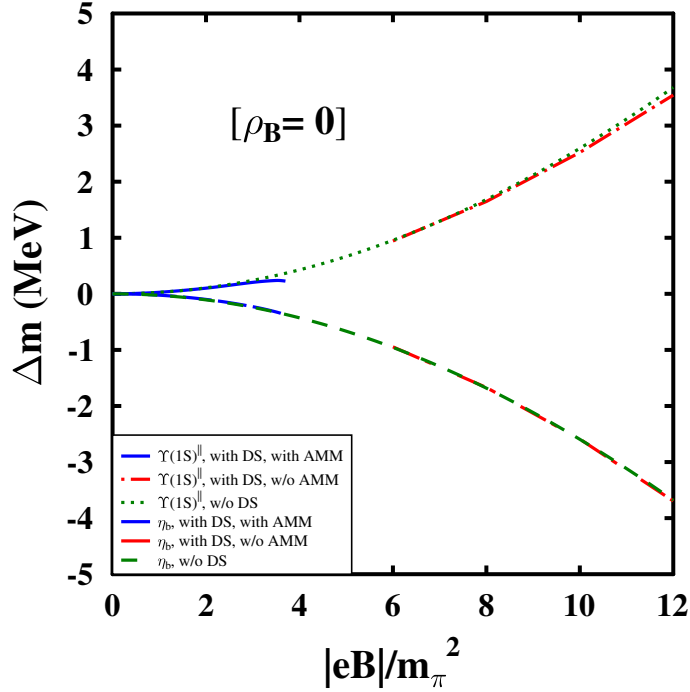


FIG. 19: Mass shifts (in MeV) are plotted as a function of $|eB|$ (in units of m_π^2), by considering the spin-mixing effects between $\Upsilon^{\parallel}(1S)$ and η_b states of S -wave bottomonium. Mixing effects are calculated with and without the Dirac sea (DS) contribution at $\rho_B = 0$.

accounting for the Dirac sea effects. The medium effects are incorporated through the scalar and twist-2 gluon condensates, calculated in terms of the medium modified scalar dilaton field, χ , and other scalar fields (σ , ζ , δ), within the chiral effective model. The effects of magnetic field coming from the Landau energy levels of protons and the non-zero anomalous magnetic moments of the nucleons, in the nuclear matter. In this work, the contribution of magnetized Dirac sea is also incorporated through the scalar densities of nucleons within the chiral effective model. Appreciable modifications in the condensates are obtained due to the Dirac sea effect along with the Landau level contribution of protons, in comparison to the case when no Dirac sea effect is considered. At zero density, the contribution of magnetic field is realized only through the magnetized Dirac sea, with no effect from the Landau energy levels of protons. The nonzero anomalous magnetic moments (AMMs) of protons and neutrons have significant effects on the in-medium masses, accounting for the

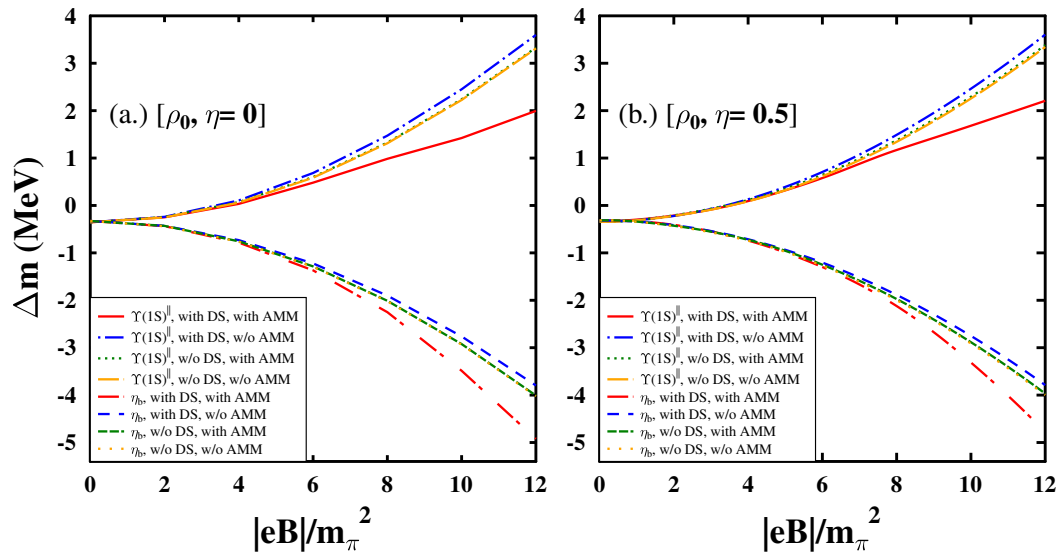


FIG. 20: Mass shifts (in MeV) are plotted as a function of $|eB|/m_\pi^2$ by considering the spin-mixing between ($\Upsilon^\parallel(1S)$ - η_b) states, at $\rho_B = \rho_0$. Mixing effects are calculated with and without DS contribution, in plot (a.) for symmetric ($\eta = 0$) and plot (b.) for asymmetric ($\eta = 0.5$) matter.

Dirac sea effect at finite magnetic field. In-medium masses of the charmonium and bottomonium ground states, accounting for the Dirac sea effects, are observed to decrease with increasing magnetic field, at finite density matter ($\rho_B = \rho_0$), when AMMs are non-zero, but show opposite behavior (increasing mass with $|eB|$) for zero AMMs of the nucleons. Thus, magnetic fields have significant contribution on the in-medium properties (masses and hence on the decay widths) of heavy quarkonia, when considering the Dirac sea effect. The magnetic fields have dominant contribution on the masses of $1S$ -wave states through the pseudoscalar-vector (PV) mixing between the longitudinal component of vector and the pseudoscalar states, which leads to an upward (downward) shifts in the masses of J/ψ^\parallel (η_c) and $\Upsilon^\parallel(1S)$ (η_b). This might be observed as a quasi-peak at the masses of m_{η_c} and m_{η_b} , in the dilepton spectra, as well as, can affect the production of heavy quarkonia and the open heavy flavor mesons, in the non-central, ultra-relativistic heavy ion collision experiments at RHIC, LHC where huge magnetic fields are generated.

Acknowledgments

Amruta Mishra acknowledges financial support from Department of Science and Technology (DST), Government of India (project no. CRG/2018/002226) and Ankit Kumar, from University Grants Commission (UGC), Government of India (Ref. 1279/(CSIR-UGC NET June 2017)).

- [1] A. Hosaka, T. Hyodo, K. Sudoh, Y. Yamaguchi, S. Yasui, *Prog. Part. Nucl. Phys.* **96**, 88 (2017).
- [2] D. Kharzeev, L. McLerran and H. Warringa, *Nucl. Phys. A* **803**, 227 (2008).
- [3] K. Fukushima, D. E. Kharzeev and H. J. Warringa, *Phys. Rev. D* **78**, 074033 (2008).
- [4] V. Skokov, A. Y. Illarionov and V. Toneev, *Int. J. Mod. Phys. A* **24**, 5925 (2009).
- [5] W. T. Deng and X.G.Huang, *Phys.Rev. C* **85**, 044907 (2012).
- [6] K. Tuchin, *Adv. High Energy Phys.* **2013**, 490495 (2013).
- [7] E. Eichten, K. Gottfried, T. Kinoshita, K. D. Lane, and T. M. Yan, *Phys. Rev. D* **17**, 3090 (1978).
- [8] E. Eichten, K. Gottfried, T. Kinoshita, K. D. Lane, and T. M. Yan, *Phys. Rev. D* **21**, 203 (1980).
- [9] S. F. Radford and W. W. Repko, *Phys. Rev. D* **75**, 074031 (2007).
- [10] Frank Klingl, Sungsik Kim, Su Houn Lee, Philippe Morath, and Wolfram Weise, *Phys. Rev. Lett.* **82**, 3396 (1999).
- [11] Sugsik Kim, Su Houn Lee, *Nucl. Phys. A* **679**, 517 (2001).
- [12] Su Houn Lee and Che Ming Ko, *Phys. Rev. C* **67**, 038202 (2003).
- [13] Arvind Kumar and Amruta Mishra, *Phys. Rev. C* **82**, 045207 (2010).
- [14] Amruta Mishra, Pallabi Parui, Ankit Kumar, and Sourodeep De, arXiv:1811.04622 [nucl-th] (2019).
- [15] Pallabi Parui, Sourodeep De, Ankit Kumar, and Amruta Mishra, arXiv:2104.05471 [hep-ph] (2021).
- [16] R. Molina, D. Gamermann, E. Oset, and L. Tolos, *Eur. Phys. J A* **42**, 31 (2009); L. Tolos, R. Molina, D. Gamermann, and E. Oset, *Nucl. Phys. A* **827**, 249c (2009).

- [17] G. Krein, A. W. Thomas and K. Tsushima, Prog. Part. Nucl. Phys. **100**, 161 (2018).
- [18] G. Krein, A. W. Thomas and K. Tsushima, Phys. Lett. B **697**, 136 (2011).
- [19] Amal Jahan C.S., Shivam Kesarwani, Sushruth Reddy P., Nikhil Dhale, and Amruta Mishra, arXiv:1807.07572 (nucl-th).
- [20] Amal Jahan CS, Nikhil Dhale, Sushruth Reddy P, Shivam Kesarwani, Amruta Mishra, Phys. Rev. C **98**, 065202 (2018).
- [21] Amruta Mishra and Divakar Pathak, Phys. Rev. C **90**, 025201 (2014).
- [22] Amruta Mishra, S.P. Misra, Phys. Rev. C **102**, 045204 (2020).
- [23] Amruta Mishra, S.P.Misra, Phys. Rev. C **95**, 065206 (2017).
- [24] S. Cho, K. Hattori, S. H. Lee, K. Morita and S. Ozaki, Phys. Rev. D **91**, 045025 (2015).
- [25] J. Schechter, Phys. Rev. D **21**, 3393 (1980).
- [26] D. Kharzeev, K. Landsteiner, A. Schmitt, and H.-U. Yee, Lect. Notes Phys. **871**, 1 (2013).
- [27] M. D’Elia, S. Mukherjee, and F. Sanfilippo, Phys. Rev. D **82**, 051501 (2010).
- [28] D. Kharzeev, Ann. Phys. (N.Y.) **325**, 205 (2010); K. Fukushima, M. Ruggieri, and R. Gatto, Phys. Rev. D **81**, 114031 (2010).
- [29] A. J. Mizher, M.N. Chenodub, and E. Fraga, Phys. Rev. D **82**, 105016 (2010).
- [30] F. Preis, A. Rebhan, and A. Schmitt, Lect. Notes Phys. **871**, 51 (2013).
- [31] D. P. Menezes, M. Benghi Pinto, S. S. Avancini, and C. Providencia, Phys. Rev. C **80**, 065805 (2009); D.P. Menezes, M. Benghi Pinto, S. S. Avancini, A. P. Martinez, and C. Providencia, Phys. Rev. C **79**, 035807 (2009).
- [32] Bhaswar Chatterjee, Hiranmaya Mishra, and Amruta Mishra, Phys. Rev. D **84**, 014016 (2011).
- [33] Alexander Haber, Florian Preis, and Andreas Schmitt, Phys. Rev. D **90**, 125036 (2014).
- [34] Arghya Mukherjee, Snigdha Ghosh, Mahatsab Mandal, Sourav Sarkar, and Pradip Roy, Phys. Rev. D **98**, 056024 (2018).
- [35] G. S. Bali, F. Bruckmann, G. Endrodi, F. Gruber, and A. Schaefer, J. High Energy Phys. 04 (2013) 130.
- [36] Arata Hayashigaki , Phys. Lett. B **487**, 96 (2000); T. Hilger, R. Thomas and B. Kämpfer, Phys. Rev. C **79**, 025202 (2009); T. Hilger, B. Kämpfer and S. Leupold, Phys. Rev. C **84**, 045202 (2011); S. Zschocke, T. Hilger and B. Kämpfer, Eur. Phys. J. A **47** 151 (2011).
- [37] Z-G. Wang and Tao Huang, Phys. Rev. C **84**, 048201 (2011); Z-G. Wang, Phys. Rev. C **92**, 065205 (2015).

- [38] P. Gubler, K. Hattori, S. H. Lee, M. Oka, S. Ozaki and K. Suzuki, Phys. Rev. D **93**, 054026 (2016).
- [39] Divakar Pathak and Amruta Mishra, Int. J. Mod. Phys. E **23**, 1450073 (2014).
- [40] Divakar Pathak and Amruta Mishra, Phys. Rev. C **91**, 045206 (2015).
- [41] Sushruth Reddy P, Amal Jahan CS, Nikhil Dhale, Amruta Mishra, J. Schaffner-Bielich, Phys. Rev. C **97**, 065208 (2018).
- [42] Nikhil Dhale, Sushruth Reddy P, Amal Jahan CS, Amruta Mishra, Phys. Rev. C **98**, 015202 (2018).
- [43] T. Hatsuda, S.H. Lee, Phys. Rev. C **46**, R34, (1992).
- [44] Amruta Mishra, Phys. Rev. C **91** 035201 (2015).
- [45] Amruta Mishra, Ankit Kumar, Pallabi Parui, Sourodeep De, Phys. Rev. C **100**, 015207 (2019).
- [46] Amruta Mishra, S.P. Misra, Int.J.Mod.Phys.E **31** (2022) 06, 2250060.
- [47] Amruta Mishra and S. P. Misra, Int. J. Mod. Phys.E **30** (2021) 08, 2150064.
- [48] A. Mishra, A. Jahan CS, S. Kesarwani, H. Raval, S. Kumar, and J. Meena, Eur. Phys. J. A **55** 99 (2019).
- [49] C. S. Machado, F. S. Navarra. E. G. de Oliveira and J. Noronha, Phys. Rev. D **88**, 034009 (2013).
- [50] C. S. Machado, R.D. Matheus, S.I. Finazzo and J. Noronha, Phys. Rev. D **89**, 074027 (2014).
- [51] K. Suzuki and S. H. Lee, Phys. Rev. C **96**, 035203 (2017).
- [52] R. J. Furnstahl, T. Hatsuda and Su H. Lee, Phys. Rev. D **42**, 5 (1990).
- [53] Young-Ho Song, S.H. Lee, K. Morita, Phys. Rev. C **79**, 014907 (2009).
- [54] K. Morita and S.H. Lee, Phys. Rev. Lett **100**, 022301 (2008); K. Morita and S.H. Lee, Phys. Rev. C **77**, 064904 (2008);
- [55] S. Cho, K. Hattori, S. H. Lee, K. Morita and S. Ozaki, Phys. Rev. Lett. **113**, 172301 (2014).
- [56] J. Alford and M. Strickland, Phys. Rev. D **88**, 105017 (2013).
- [57] P. Papazoglou, D. Zschesche, S. Schramm, J. Schaffner-Bielich, H. Stöcker, and W. Greiner, Phys. Rev. C **59**, 411 (1999).
- [58] S. Weinberg, Phys. Rev. **166** 1568 (1968).
- [59] S. Coleman, J. Wess, B. Zumino, Phys. Rev. **177** 2239 (1969); C.G. Callan, S. Coleman, J. Wess, B. Zumino, Phys. Rev. **177** 2247 (1969).
- [60] W. A. Bardeen and B. W. Lee, Phys. Rev. **177** 2389 (1969).

- [61] A. Mishra, K. Balazs, D. Zschesche, S. Schramm, H. Stöcker, and W. Greiner, Phys. Rev. C **69**, 024903 (2004).
- [62] D. Zschesche, A. Mishra, S. Schramm, H. Stöcker and W. Greiner, Phys. Rev. C **70**, 045202 (2004).
- [63] Erik K. Heide, Serge Rudaz and Paul J. Ellis, Nucl. Phys. A **571**, (2001) 713.
- [64] A. Broderick, M. Prakash and J.M.Lattimer, Astrophys. J. **537**, 351 (2002).
- [65] A.E. Broderick, M. Prakash and J. M. Lattimer, Phys. Lett. B **531**, 167 (2002).
- [66] F. X. Wei, G. J. Mao, C. M. Ko, L. S. Kisslinger, H. Stöcker, and W. Greiner, J. Phys. G, Nucl. Part. Phys. **32**, 47 (2006).
- [67] Guang-Jun Mao, Akira Iwamoto, Zhu-Xia Li, Chin. J. Astrophys. **3**, 359 (2003).
- [68] M. Pitschmann and A. N. Ivanov, arXive : 1205.5501 (math-ph).
- [69] V. Dexheimer, R. Negreiros, S. Schramm, Eur. Phys. Journal A **48**, 189 (2012).
- [70] V. Dexheimer, B. Franzon and S. Schramm, Jour. Phys. Conf. Ser. **861**, 012012 (2017).
- [71] R. M. Aguirre and A. L. De Paoli, Eur. Phys. J. A **52**, 343 (2016).
- [72] S.H. Lee and K. Morita, Phys. Rev. D **79**, 011501(R) (2009); S.H.Lee and K. Morita, Pramana Journal of Physics **72**, 97 (2009); K. Morita and S.H. Lee, Phys. Rev. C **85**, 044917 (2012).
- [73] Thomas D. Cohen, R. J. Furnstahl and David K. Griegel, Phys. Rev. C **45**, 1881 (1992).
- [74] L. J. Reinders, H. R. Rubinstein, and S. Yazaki, Nucl. Phys. B **186**, 109 (1981).
- [75] L. J. Reinders, H. R. Rubinstein, and S. Yazaki, Physics reports **127**, 1 (1985).
- [76] P.A. Zyla et al. (Particle Data Group), Prog. Theor. Exp. Phys. **2020**, 083C01 (2020).